University of Nebraska - Lincoln
DigitalCommons@University of Nebraska - Lincoln

Student Research Projects, Dissertations, and Theses - Chemistry Department

Chemistry, Department of

8-2011

High Yield Synthesis of Positron Emission Tomography Ligands for Metabotropic Glutamate Receptor Imaging

Saraanne E. Hitchcock
University of Nebraska-Lincoln, shitchcock@huskers.unl.edu

Follow this and additional works at: http://digitalcommons.unl.edu/chemistrydiss

Part of the Medicinal-Pharmaceutical Chemistry Commons, and the Organic Chemistry Commons

Hitchcock, Saraanne E., "High Yield Synthesis of Positron Emission Tomography Ligands for Metabotropic Glutamate Receptor Imaging" (2011). *Student Research Projects, Dissertations, and Theses - Chemistry Department*. 25.
http://digitalcommons.unl.edu/chemistrydiss/25

This Article is brought to you for free and open access by the Chemistry, Department of at DigitalCommons@University of Nebraska - Lincoln. It has been accepted for inclusion in Student Research Projects, Dissertations, and Theses - Chemistry Department by an authorized administrator of DigitalCommons@University of Nebraska - Lincoln.

Chemistry, Department of

Student Research Projects, Dissertations, and Theses - Chemistry Department

University of Nebraska - Lincoln *Year* 2011

High Yield Synthesis of Positron Emission Tomography Ligands for Metabotropic Glutamate Receptor Imaging

Saraanne E. Hitchcock
University of Nebraska-Lincoln, shitchcock@huskers.unl.edu

This paper is posted at DigitalCommons@University of Nebraska - Lincoln.
http://digitalcommons.unl.edu/chemistrydiss/1

High Yield Synthesis of Positron Emission Tomography Ligands for Metabotropic Glutamate Receptor Imaging.

By

Saraanne E. Hitchcock

A THESIS

Presented to the Faculty of

The Graduate College at the University of Nebraska

In Partial Fulfillment of Requirements

For the Degree of Master of Science

Major: Chemistry

Under the Supervision of Professor Stephen G. DiMagno

Lincoln, Nebraska

August 2011

High Yield Synthesis of Positron Emission Tomography Ligands for Metabotropic Glutamate Receptor Imaging.

Saraanne E. Hitchcock, M.S.

University of Nebraska, 2011

Advisor: Stephen G. DiMagno

Positron Emission Tomography (PET) is a powerful and non-invasive imaging technique used for human and animal organ imaging. Currently, the market for PET is project to reach $5.4 billion per year by 2015.[5] This research focuses on the direct incorporation of [18F]-fluoride into PET ligands. The widespread use of PET imaging is currently frustrated, in part, by the lack of efficient fluorination chemistry.

Glutamate, one of the 20 most abundant naturally occurring amino acids, serves as a neurotransmitter in the central nervous system. Glutamate functions in this capacity by binding to ionotropic and metabotropic receptors. Metabotropic receptors are G-coupled proteins that are involved in many disorders such as Parkinson’s disease, anxiety, depression and addiction. This research focuses on the preparation of PET ligands for the mGluR5 subtype receptor.

3-fluoro-5-(pyridin-2-ylethynyl)benzonitrile (PEB) and 3-fluoro-5-((6-methylpyridin-2-yl)ethynyl)benzonitrile (MPEB) are the two of the drugs of interest for this research. Previously reported ^{18}F-radiolabeling techniques for the preparation of compounds of this class involved a halogenated precursor with KF in DMSO and using microwave heating. This strategy yielded approximately 4% RCY ("RCY" in this thesis refers to decay-corrected yield). We chose this class of compounds as a target because it provides an opportunity to develop synthetic [^{18}F]-fluoride methodology to make this drug widely available for neuroscience and neuromedicine.

This method developed here for fluorination of aromatic rings can be expanded to achieve incorporation of ^{18}F into aromatic amino acids. Amino acids have been known to target tumor cells specifically. In conclusion, this newly developed fluorination methodology opens a door to a variety of compounds that can be used for PET imaging studies.

ACKNOWLEDGEMENTS

First and foremost I would like to thank Dr. Stephen DiMagno for the opportunity to work in his research group. This has been a wonderful experience, both fun and challenging. I would also like to thank the members of the DiMagno research lab for support both in chemistry and outside the lab: Dr. Bijia Wang, ShriHarsha Uppaluri, Mark Cradduck, Linlin Qin, Jayson Kempinger, Kiel Neumann and Sarah Kruse. A special thanks to my best friend and partner Joshua Lovell, thank you for supporting me in chemistry and everything else. Also like to thank Dr. K.C. Russell at Northern Kentucky University for introducing me to research in organic chemistry, and how exciting it can be to produce new molecules “from scratch.”

TABLE OF CONTENTS

ACKNOWLEDGEMENTS……………………………………………………………….4

TABLE OF CONTENTS……………………………………………………………..5

LIST OF FIGURES………………………………………………………………….7

LIST OF SCHEMES…………………………………………………………………8

LIST OF TABLES……………………………………………………………………9

CHAPTER 1-Introduction

1.1 PET………………………………………………………………………………..10

1.2 Metabotropic Glutamate Receptors……………………………………………13

1.3 Antagonists of mGluR5………………………………………………………….15

CHAPTER 2

2.1 Possible Fluorination Techniques………………………………………………18

2.2 Using ^{18}F as a Labeling Agent…………………………………………….…21

2.3 Diaryliodonium Salts……………………………………………………………22

2.4 Established Protocol for mGluR5 Synthesis…………………………………...24

2.5 New Synthetic Approach for F-PEB……………………………………………25

CHAPTER 3-Conclusions and Future Work

3.1 Expansion of Methodology to Aromatic Amino Acids…….……………………..30

REFERENCES……………………………………………..………………………33

LIST OF FIGURES

Figure 1. Commonly used radiotracers for PET imaging……………………………….10

Figure 2. Theory of PET imaging…………………………………………………….11

Figure 3. Graphical representation of mGlu Receptor…………………………………..15

Figure 4. Non competitive mGluR5 antagonists……………………………………...16

Figure 5. Radioligands for mGluR5 subtype receptor used in PET imaging…………...17

Figure 6. Metal-catalyzed fluorination………………………………………………19

Figure 7. Method for isolation of ^{18}F ion from cyclotron……………………………….22

Figure 8. Current amino acid analogues used for PET imaging……………………...31

Figure 9. Possible aromatic amino acid radiotracers…………………………………31

LIST OF SCHEMES

Scheme 1. $^{18}F_2$ production via electrophilic means; incorporation of $^{18}F_2$ into DOPA....20

Scheme 2. Some common uses of diaryliodonium salts…………………………………...23

Scheme 3. Synthetic approach for radio-labeled PEB…………………………………..24

Scheme 4. Some examples of radiofluorination with diaryliodonium salts……………..24

Scheme 5. Preparation of 3-fluoro-5-(pyridin-2-ylethynyl)benzonitrile………………...25

Scheme 6. Stannylation of 3-fluoro-5-(pyridin-2-ylethynyl)benzonitrile……………….26

Scheme 7. Diaryliodonium Chemistry of PEB………………………………………….27

Scheme 8. Fluorination procedure for PEB……………………………………………..27

LIST OF TABLES

Table 1. Properties of commonly used positron-emitting radionuclides………………..10

CHAPTER ONE

Positron emission tomography (PET) is a non-invasive imaging technique used to visualize physiological and biological processes in real time.[1] Compounds are tagged with a radioactive isotope, allowed to diffuse to the appropriate biological target and pinpointed by determining the source of the emitted radiation. Figure 1 shows commonly used PET radiotracers and their uses.

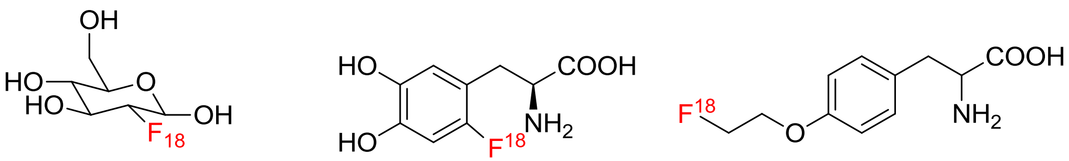

[^{18}F]FDG
metabolism
marker

[^{18}F]FDOPA
brain dopamine
metabolism

[^{18}F]FET
Tumor Location

Figure 1. Commonly used radiotracers for PET imaging.[1]

In PET, the radionuclide label decays by emitting a positron, a positively charged particle of negative mass. The positron is emitted with significant kinetic energy, but it slows down within ~ 1 mm as it collides with an electron, after which it annihilates an electron. This matter-antimatter reaction produces two gamma rays (γ-rays) emitted at 180^{o}, as shown in Figure 2. The gamma-rays are detected by a scintillation detector, and the simultaneity of the detection events is used to determine the path of the emitted gamma ray. Localization of the drug is determined by counting the number of rays passing through various regions of the space within the detector. Because PET provides no structural information, images are often coupled with a CT scan to give physiological landmarks.

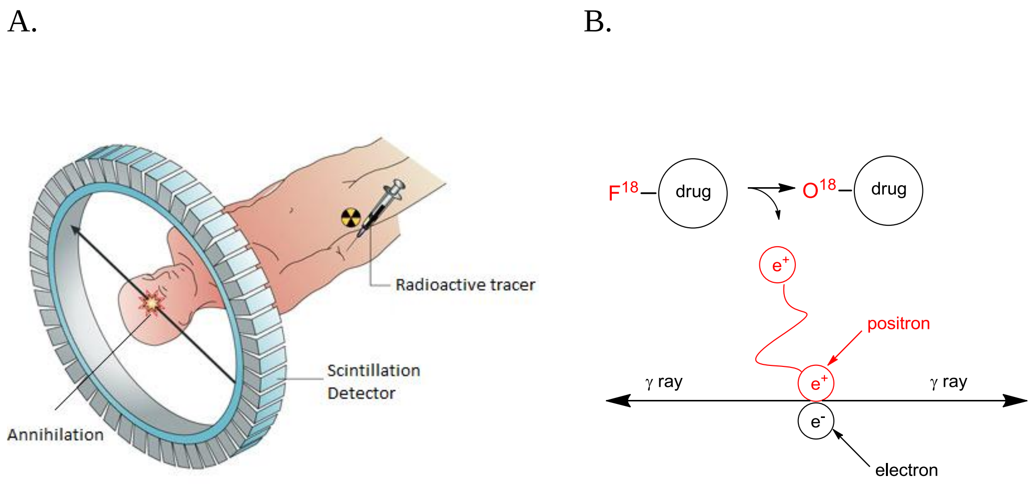

Figure 2. PET imaging. A. Schematic diagram showing the process and apparatus for collecting a pet scan. Modified from Nature Reviews, 4, **June 2004**, 457-469. B. Cartoon showing the nuclear processes leading to the production of gamma rays.

Several radioactive isotopes used for PET imaging are listed in Table 1. The most commonly used radionuclides are ^{11}C, ^{13}N, ^{15}O and ^{18}F.[2] These radionuclides are desirable for radiopharmaceuticals because they are easy to incorporate into ligands without perturbing significantly the ligand's affinities for their biological receptors. ^{11}C appears to be an excellent candidate for PET imaging. However, the extremely short half-life (20.4 minutes), severely constrains the types of synthetic reactions that can be used to introduce it. While using a radionuclide with a short half-life seems counterintuitive; ^{13}N (10 min) and ^{15}O (2 min), have been applied to PET-based monitoring of myocardial blow flood and cerebral blood flow, respectiviey.[3] Some advantages of using a short half-life radionuclide are that the overall dose exposure of both patient and clinicians are low, and allows for repeat imaging experiments to be performed in a single day without requiring a patient to stay overnight at a hospital.

^{18}F-Fluorine is in some sense an ideal radioactive isotope for PET imaging. ^{18}Fluorine has a half-life (110 min) that allows for moderately complex synthetic transformations to be performed. The half-life is sufficiently long to permit even a multistep synthesis, while still providing a highly radioactive compound. The half-life is sufficient to allow transportation of the drug to a clinical setting away from the original cyclotron laboratory. Another reason that ^{18}F is such an attractive candidate for PET imaging is due to the emitting of low energy positron upon decay (0.64 MeV), the positron (β+) travels a short distance before it is annihilated (~ 1 mm).

Isotope	**Half-life**	**Maximum Energy (MeV)**	**Mode of Decay (%)**	**Theoretical Specific activity (GBq/umol)**
^{18}F	110 min	0.64	β + (97%) EC (3%)	6.3×10^{4}
^{11}C	20.3 min	0.97	β+ (99%)	3.4×10^{5}
^{13}N	10 min	1.20	β+ (100%)	7.0×10^{5}
^{15}O	2 min	1.74	β+ (100%)	3.4×10^{6}
^{76}Br	16 hrs	4.0	β+ (57%) EC (43%)	7.2×10^{3}
^{124}I	41.8 days	2.14	β+ (25%) EC (75%)	1.15×10^{3}
^{68}Ga	68.1 min	1.90	β+ (89%) EC (11%)	1.02×10^{5}
^{64}Cu	12.7 hrs	0.655	β+ (19%) EC (41%) β+ (40%)	9.13×10^{3}

Table 1. Properties of Commonly Used Positron-Emitting Radionuclides[3]

Structurally, fluorine is advantageous to incorporate into molecules of interest. In chemical transformations, fluorine can be used to replace a hydrogen; although it may be more advantageous to replace an oxygen or a hydroxyl group. Fluorine and oxygen are sterically similar with Van der Waals radii of 1.52 and 1.47, respectively.[1] Fluorine and oxygen are more electronically similar than fluorine and hydrogen; with electronegativity scores of 2.20 (H), 3.44 (O) and 3.98 (F).[1] Although in some cases changing the polarity of a bond (C-H to C-F) can increase the potency of the drug.[4]

Currently, the dollar value of the PET market is projected to reach $5.4 billion in Europe and the United States by 2015.[5]

1.2 Metabotropic Glutamate Receptors

L-Glutamate is a major excitatory neurotransmitter in the central nervous system (CNS). Glutamate is regulated by two types of glutamate receptors; ionotropic and metabotropic. These two protein receptors can be further categorized into two types based upon their mechanisms of action.[6] Ionotropic glutamate receptors are ligand-gated ion channels.[6] The ion channels allow the transport of K^+, Na^+ and Ca^{2+}. The flow of cations causes the neuron to become polarized and send signals down the neuron. Metabotropic glutamate receptors (mGluR) are G-coupled protein receptors; this receptor type is responsible for modulation of synaptic transmission.[7] This family includes $GABA_b$, pheromone, and Ca^{2+} sensing receptors.

There are eight members (mGluR1-8) of the mGluR family. These eight proteins are distinguished on the basis of their sequence homology, second messenger coupling, and pharmacology. Group I (mGluR1 and mGluR5) couple via an alpha G-protein (Gq/G11) to phospholipase C.[8,11] Phospholipase C is an enzyme that is involved in hydrolysis of phospholipids into diacylgylcerol and the corresponding phosphorylated head group. The mechanism of this biochemical response begins with binding of glutamate to the receptor which catalyzes GTP-GDP exchange on the associated G protein; this energy transfer activates the G protein. The activated G protein then activates a specific membrane bound phospholipase C (PLC). PLC catalyzes production of two secondary messenger molecules: diacylglycerol and inositol 1,4,5-trisphosphate (IP_3).[7] IP_3 binds to receptors on the endoplasmic reticulum and causes Ca^{2+} to be released.[7] Group II (mGluR2 and mGluR3) and group III (mGluR4, 6, 7, 8) couple to a heterotrimeric G-protein (Gi/Go) to inhibit adenylyl cyclase activity.[6] Andenylyl cyclase catalyzes the production of cAMP from ATP. Most mGluR5s are located in the mammalian CNS and glial cells. Group I is mainly located in a postsynaptic portion of the neuron, while groups II and III are found in the presynaptic part of the neuron and their main function is control of neurotransmitter release.

A large, extracellular bi-lobed N terminal domain, characteristic of all mGlu receptors, is tethered with a cysteine-rich region.[9] The cleft between the bi-lobed regions is the glutamate binding site. The N-terminal domain is tethered to the seven transmembrane helical domain, that is anchored to the membrane. Glutamate binds to the extracellular bi-lobed domain. The seven transmembrane helical domain contains binding sites for noncompetitive positive and negative allosteric ligands. A noncompetitive ligand is defined as one that does not bind at the same site as the endogenous glutamate, and therefore does and there for does not compete directly with glutamate.

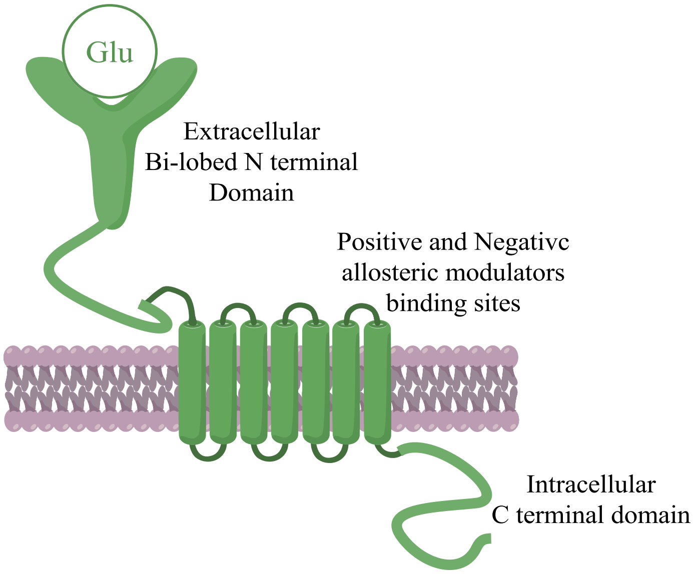
Glu
Extracellular
Bi-lobed N terminal
Domain
Positive and Negativc
allosteric modulators
binding sites
Intracellular
C terminal domain

Figure3.[9] Cartoon of an mGlu receptor.

On the basis of the widespread distribution of mGluR5 throughout CNS, particularly in regions that play essential roles in motor coordination and movement, it is thought that dysfunction of these receptors is implicated in neurological diseases, including anxiety, epilepsy and Alzheimer's.[10] For example, Parkinson's is linked to an overexpression of mGluR5, so it is believed that inhibiting this receptor may offer an opportunity for treatment of this disease.[10] Currently, several pharmaceuticals companies(Pfizer, Eli Lilly & Co, and Novartis) are exploring Parkinson's therapeutic drug discovery efforts featuring mGluR5 as the target receptor.[9]

1. 3 mGluR5 Antagonists

Glutamate, the endogenous ligand for mGluR5, is actually a poor starting point for developing a specific PET imaging agent because glutamate binds to ionotropic and metabotropic receptors, and would not have receptor specificity. Research was focused on noncompetitive antagonists of mGluR5. These types of compounds are advantageous due to the fact they will not compete with endrogenous glutamate and not decrease the ligand-receptor sensitivity.[10] Figure 4 shows noncompetitive mGluR5 antagonists.

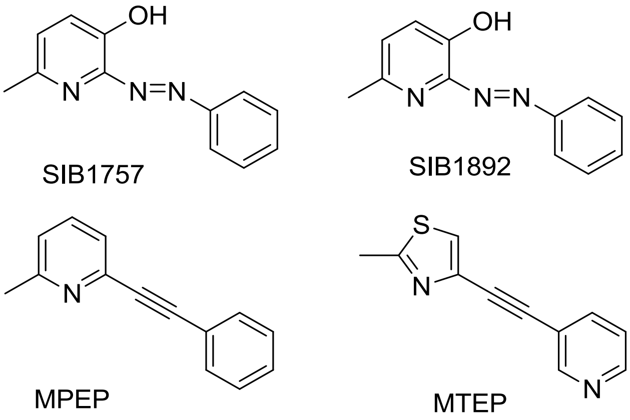

SIB1757

SIB1892

MPEP

MTEP

Figure 4. Noncompetitive mGluR5 antagonists

High throughput screening of a compound library yielded the first noncompetitive mGluR5 antagonists in 1999. This work was performed by Mark Varney at SIBIA Neurosciences, gave the compounds SIB1757 and SIB1892, shown in Figure 4.[12] These compounds are selective, noncompetitive antagonists, and do not bind to the glutamate receptor site in the N-terminal region of the receptor. This binding property helps make these compounds more selective for the mGluR5. SIB1757 and SIB1892 were used as a starting point for medicinal chemistry. It was determined that replacement of the double bond between the aromatic rings with a triple bond yielded higher antagonist activity.[10] These new structures, MPEP and MTEP do not resemble glutamate at all, feature appropriate lipophility, and have good blood-brain barrier permeablilty.[10]

With an appropriate set of mGluR5 antagonists identified, PET could be used to image glutamate receptor distribution in the brain. Efforts were put toward heteroaryl acetylenes labeled with ^{18}F or ^{11}C. Figure 5 shows the insertion of radioactive nuclides into targets reported to have the best binding profile for PET imaging studies.[10] Two compounds that are of interest to the DiMagno lab are 3-fluoro-5-(pyridin-2-ylethynyl)benzonitrile (PEB) and 3-fluoro-5-((2-methylthiazol-4-yl)ethynyl)benzonitrile (MTEB). [^{18}F]-PEB is sufficiently lipophilic to cross the blood brain barrier, with a LogD (lipophilicity coefficient) value of 2.8. A LogD value between 2 and 3 is considered optimal for penetration of a compound in the brain.[10] [^{18}F]-PEB is extremely potent; the ki value for the mGluR5 protein is 0.2 nM. A metabolism study was performed on [^{18}F]-PEB and showed that 78% of the injected radioactivity (decay corrected) was found in the brain 30 minutes after administration of the radiotracer.

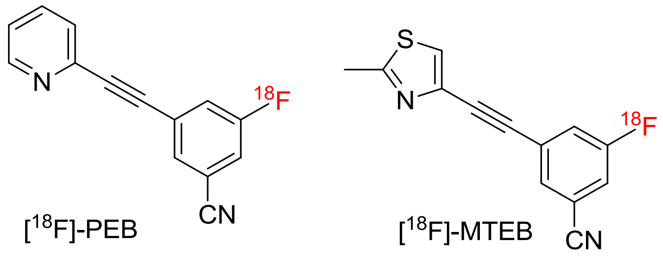

Figure 5.PET radioligands for the mGluR5 subtype receptor.

The biochemistry of PEB has been investigated extensively.[14,15] The precursors to the radioactive drug ([^{18}F]-PEB) have been synthesized in high yields, but currently employed fluorination techniques have produced [^{18}F]-labeled PEB and MTEB in only 4 ± 0.9% and 4 ± 0.6%, respectively.[13] In PEB and MTEB we have clearly identified, potentially valuable radioligands for PET neuroimaging, but there are no effective synthetic methodologies for preparing them. This thesis describes my approach to preparing these compounds using novel diaryliodonium salt precursors.

CHAPTER TWO

2.1 Possible Fluorination Techniques

Approximately one third of all currently prescribed pharmaceuticals contain at least one fluorine atom. Most often fluorine substituents are incorporated to control drug catabolism from cytochrome p450 activity. Fluorination of oxidatively sensitive aromatic rings is a particularly common tool of the trade to enhance lifetime. Typical fluorination methods require harsh conditions which are not compatible with many functional groups; to utilize these methods scientist install the fluorine substituents early in the synthesis. Some traditional methods to fluorinate aromatic rings include Balz-Schiemann (B.S) and nucleophilic substitution (SnAr) of electron-deficient arylhalides with KF.[15] The Balz-Schiemann reaction converts aryl amines to aryl fluorides, via a diazonium salt intermediate. Preparatory of the aryl diazonium salt typically requires acidic conditions, which may be problematic with particular functional groups. For synthesis of PET radiotracers, incorporation of [^{18}F] fluoride must be performed toward the end of the synthesis because the short half-life of the isotope (110 min) precludes time consuming, multistep procedures subsequent to fluorination. Some new methodologies have been developed recently that describe late stage introduction of fluoride into electron-rich aromatic rings.

One possible method to increase the fluorination yield is to utilize transition metal catalysts, specifically palladium. Figure 5 shows a proposed palladium-catalyzed fluorination mechanism recently published by Buchwald and co-workers.[16] This method has a tolerance of many functional groups which broadens the substrate scope to highly complex targets. While the idea of a catalytic system seems attractive as a means to fluorinate aromatic rings it is currently only practical for ^{19}F incorporation. This process requires high catalyst loading, and a long reaction time (12 h), which is not compatible with ^{18}F incorporation.

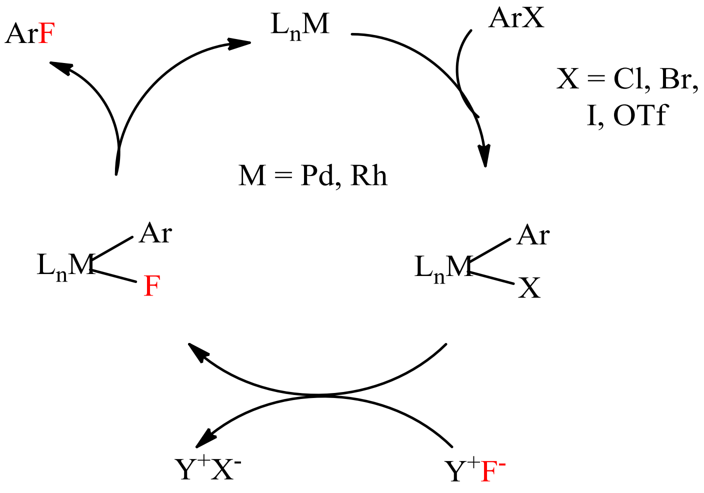

Figure 6.[16] Metal catalyzed fluorination.

Electrophilic fluorination procedures have been used for the preparation of PET radioligands.[4] Electrophilic methods rely on the generation of ^{18}F-labeled F_2. [$^{18}F_2$] is produced via bombardment of gas containing neon and 0.1% $^{19}F_2$ with deuterons. Scheme 1 shows the nuclear reaction used to produce electrophilic ^{18}F, and application of $^{18}F_2$ in a fluorodemetalation reaction to produce [^{18}F]FDOPA.[17]

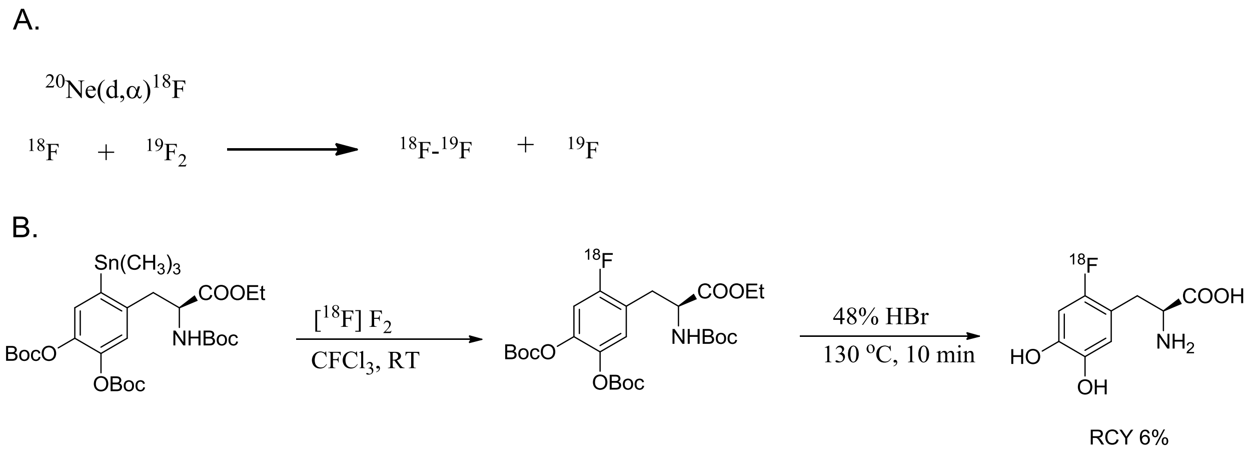
A.
20Ne(d,α)18F
18F + 19F2
18F-19F + 19F
B.
Sn(CH3)3
COOEt
NHBoc
BocO
OBoc
[18F] F2
CFCl3, RT
18F
COOEt
NHBoc
BocO
OBoc
48% HBr
130 °C, 10 min
18F
COOH
NH2
HO
OH
RCY 6%

Scheme 1. A. Process by which electrophilic $^{18}F_2$ is produced. B. Incorporation of $^{18}F_2$ into DOPA, used for PET imaging of brain dopamine metabolism.

There is an inherent problem associated with electrophilic fluorination: the specific activity of the [^{18}F]-fluorinated radioligands is always low. This problem arises because of two reasons; one, the [^{18}F]-labeled F_2 only has one ^{18}F atom, thus the maximum achievable radiochemical yield is only 50%[3], and two, the concentration of gas is 1,000-10,000 times that of the ^{18}F atom concentration. This dilution results in PET ligands that are contaminated with huge amounts of the ^{19}F-labeled compound. The presence of the nonradioactive PET ligand can degrade image quality and lead to secondary drug effects and toxicity.

There has been a drive to develop no-carrier added fluorination reactions to avoid the pitfalls of carrier-added fluorination. This has been achieved through the use of nucleophilic radiofluroinations.[3] The amount of radioactivity that can be produced in a commercial cyclotron by proton bombardment of an $^{18}OH_2$ target is approximately 1000 GBq (~30 Cures). Specific activity is the amount of radioactivity per mole of compound.

For per 18F-, the specific activity is on the order of 1 Curie (376 Bq) per 10 ng (~60 GBq/nanomole).

Direct introduction of no carrier-added fluoride is the reaction of choice for preparing high specific activity material. Direct nucleophilic fluorination reactions are severly limited in scope, generally the arene to be fluorinated must possess an electron-withdrawing group. The reaction must be carried out under extremely dry conditions. The fluoride ion, $^{18}F^{-}$, is a poor nucleophile in an aqueous environment. Fluoride can be activated with the addition of a cryptand and tetra-n-butylammonium salt, in most cases these are Kryptofix 2.2.2.(cryptand) and potassium carbonate (tetra-n-butylammonium salt). Nucleophilic radio-fluorinations of aliphatic systems usually follow a S_n2 mechanism in dipolar aprotic solvents. Classically, only activated (NO_2, CN, CHO, and COOR) aromatic rings were needed to incorporate the ^{18}F moiety, but not all clinically relevant biomolecules contain an activating group, there is a drive to become creative with the chemistry.

2.2 Using ^{18}F as a labeling agent

The current technique for production of ^{18}F is proton bombardment of H_2O^{18}. Following bombardment, the [18F]-fluoride is trapped on an ion exchange resin, and eluted with aqueous carbonate or bicarbonate (Figure 6). Residual water is removed by multiple azeotropic distillations with acetonitrile.

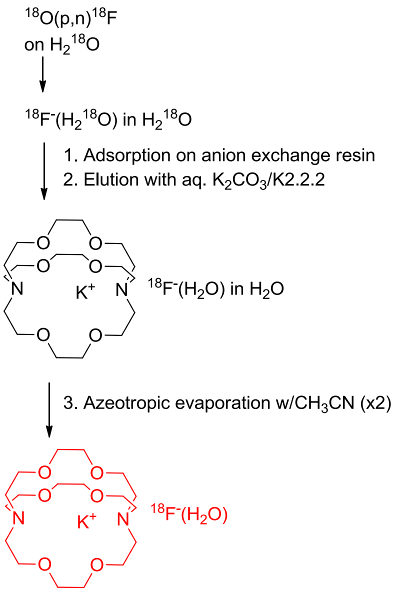

$^{18}O(p,n)^{18}F$
on $H_2{}^{18}O$
$^{18}F^-(H_2{}^{18}O)$ in $H_2{}^{18}O$
1. Adsorption on anion exchange resin
2. Elution with aq. K_2CO_3/K2.2.2
O
O
O
O
N
K^+
N
O
O
$^{18}F^-(H_2O)$ in H_2O
3. Azeotropic evaporation w/CH_3CN (x2)
O
O
O
O
N
K^+
N
O
O
$^{18}F^-(H_2O)$

Figure 7. Method for isolation of ^{18}F ion from cyclotron product.

The addition of Kriptofix 2.2.2 helps to solubilize the fluoride ion in polar aprotic solvents, and sequesters the cation to bolster the fluoride ion nucleophilicity.

2.3 Diaryliodonium salts

Diaryliodonium salts, λ^3diaryl-iodanes, were first synthesized in 1894.[18] These compounds are air and moisture stable, which make them attractive reagents in organic synthesis. Scheme 3 shows two reactions that diaryliodonium salts are commonly used in. Diaryliodonium salts can be formed as either symmetrical or unsymmetrical salts (Scheme 3.a); this avoids any selectivity issues when reductive elimination occurs. The nucleophilic displacement of the iodonium salt will reductively eliminate to the desired ring. It is believed that the iodonium salts proceed through a reductive elimination mechanism, in which the aryl-group is transferred to the nucleophile (Scheme 3.b).

Iodonium salts can act as aryl-iodides and transfer the aryl group and ligand to a metal; as in an oxidative addition.[18]

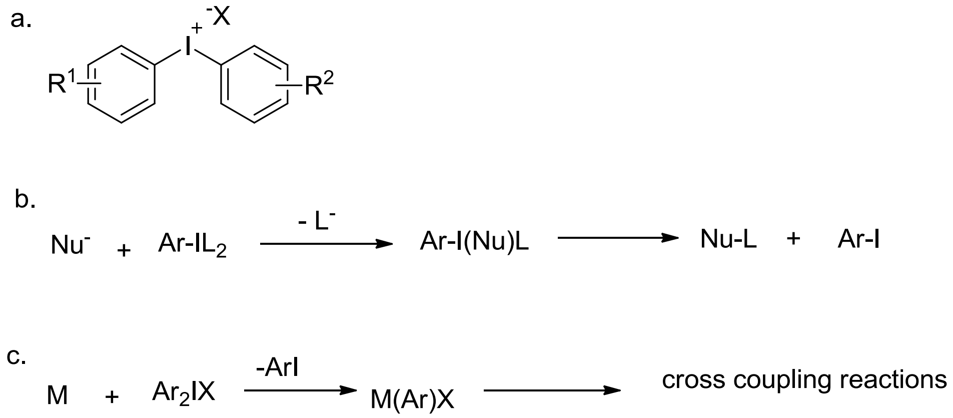

Scheme 2.[18] Some common uses for diaryliodonium salts. (a) General structure for diaryliodonium salts, X = Cl, Br, I OTf, OTs. (b) Reaction of diaryliodonium salts and nucleophiles. (c)Metal catalyzed reactions of diaryliodonium salts, yielding cross coupling products.

Reductive elimination of diaryliodonium salts would seem to be a facile way to introduce ^{18}F in an efficient and selective manner. In Scheme 4 it can be seen that this method is reported to work on several systems with diverse functionality.

It has been shown that thermal decomposition of diaryliodides favor functionalization on the electron-poor ring, while the iodine stays on the electron-rich ring.[18] The directing group in iodonium reactions can vary. Scheme 4 shows the directing group as a p-methoxy phenyl, but the directing group can be any aryl group, most notably 2-thienyl and p-cyclophane.

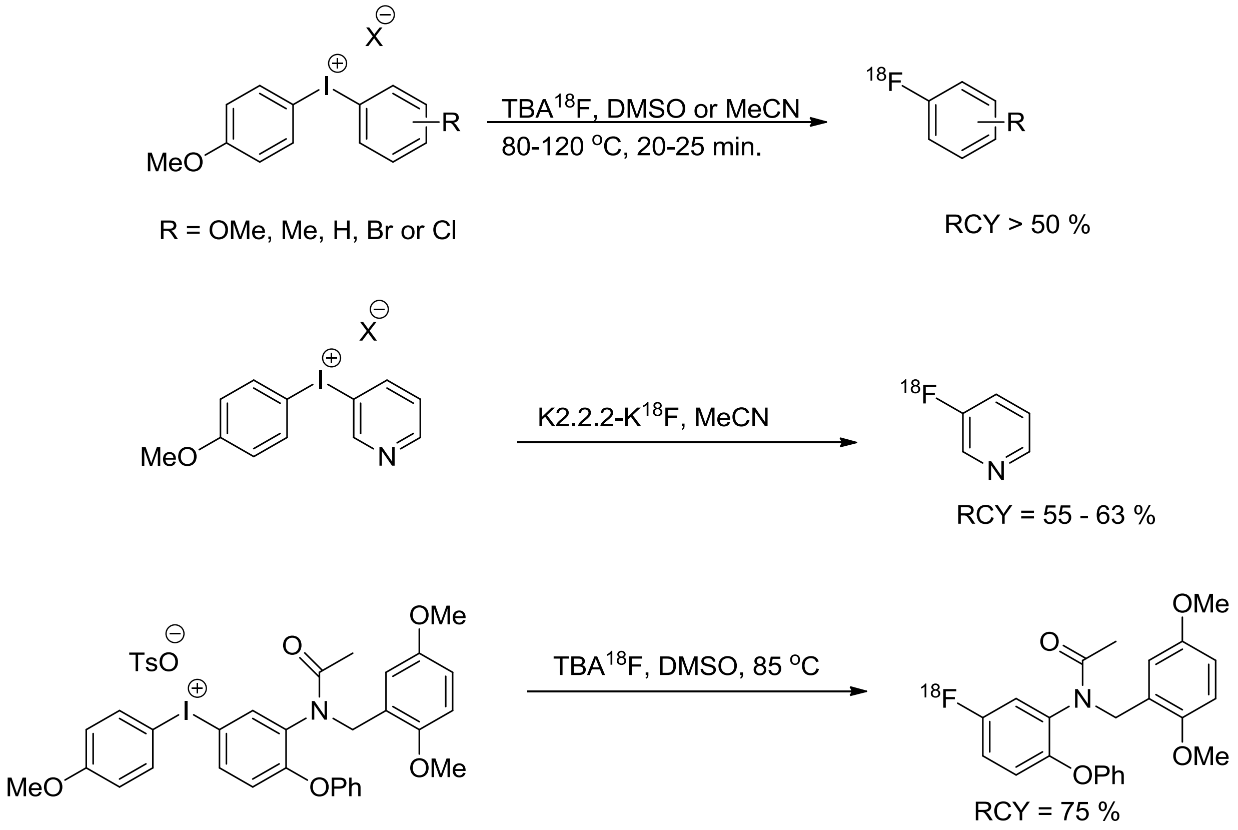
X⊖
I⊕
MeO
R
TBA18F, DMSO or MeCN
80-120 °C, 20-25 min.
18F
R
R = OMe, Me, H, Br or Cl
RCY > 50 %
X⊖
I⊕
MeO
N
K2.2.2-K18F, MeCN
18F
N
RCY = 55 - 63 %
TsO⊖
I⊕
MeO
O
N
OMe
OMe
OPh
TBA18F, DMSO, 85 °C
18F
O
N
OMe
OMe
OPh
RCY = 75 %

Scheme 3. Some examples of radiofluroination with Diaryliodonium salts.[1] RCY is decay-corrected radiochemical yield.

2.4 Established protocol for mGluR5 synthesis

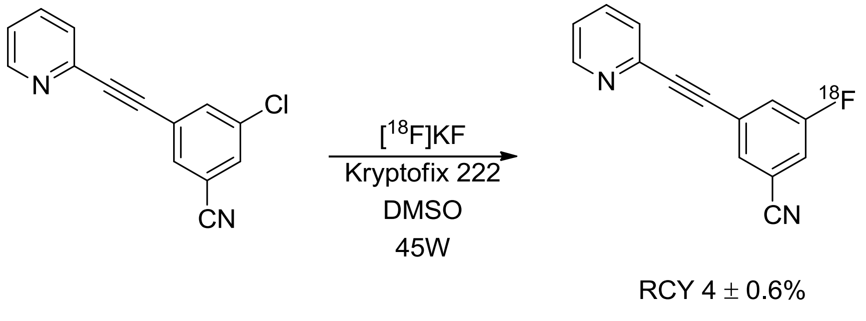
N
Cl
CN
[18F]KF
Kryptofix 222
DMSO
45W
N
18F
CN
RCY 4 ± 0.6%

Scheme 4. Synthetic approach for radio-labeled PEB.[13]

Hamill and coworkers (Merck Research Laboratories) were the first to synthesize the mGluR5 ligand. Most chemical transformations used in PET radiotracer synthesis take less than 20 minutes. While the reaction time is suitable for PET radiotracer synthesis, the yield was atrocious. This method left much ground to make up if this was to be widely utilized as a synthetically useful reaction.

2.5 New Synthetic Approach for F-PEB

There is a need for a new method for nucleophilic fluorination, one that increases yield and maintains the short reaction time. The DiMagno group has developed a method for fluorination of electron deficient aromatic rings. This method utilizes hypervalent iodine to introduce fluorine in relatively high yields (>70%). This newly developed iodonium chemistry begins with a halogenated precursor.

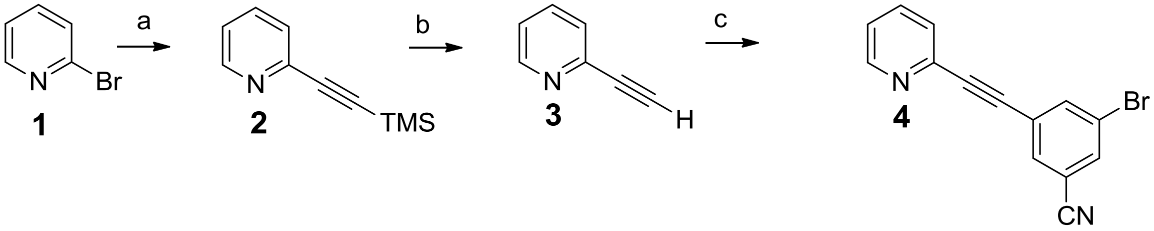

Scheme 5. The preparation of 3-bromo-5-((6-methylpyridin-2-yl)ethynyl)benzonitrile

Reagents and conditions: (a) (trimethylsilyl) acetylene, $PdCl_2(PPH_3)_2$, CuI, Et_3N, 90 °C; (b) KOH, MeOH, room temp; (c) 3,5-dibromobenzonitrile, $PdCl_2(PPh_3)_2$, CuI, Et_3N, 90 °C.

The brominated precursor of PEB (**1**, Scheme 5) was synthesized in 2005 by the Tamagnan group.[15] The commercially available starting material, 2-bromopyridine, was subjected to Sonogashira coupling with TMS-acetylene, using Pd (II). This first synthetic step took about 12 hours at 90 ^{o}C and had a very high yield, 96%. The 2-(trimethylsilylethnynyl)pyridine (**2**) product was easily purified by silica gel flash chromatrography and deprotected with KOH and MeOH, in essentially quantitative yield (**3**). A second, more challenging Sonogashira coupling reaction was performed with the deprotected alkyne and 3,5-dibromobenzonitrile. The reaction produced the desired brominated pyridinylethnylyl benzonitrile (**4**), but also a large amount of Glaser coupled diyne, which was only removed with difficulty from the desired product. To overcome this problem, the alkyne concentration was kept low in the presence of a gross excess of the dibromobenzonitrile. The alkyne was added in small aliquots over the course of several hours. Palladium catalyzed stannylation (**5**) was performed on the brominated benzonitrile precursor. An important aspect of the stannylation step that should be noted was that the reaction worked best when excess (4 equiv.) of Bu_3Sn_2 was used to eliminate cross coupling products

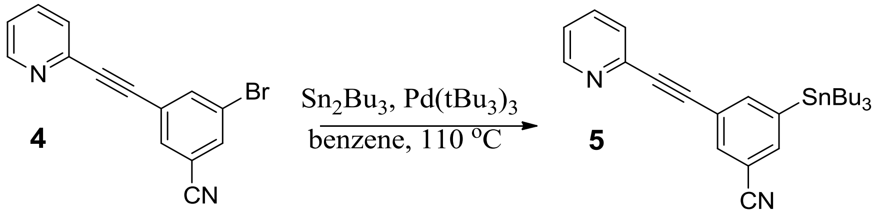

Scheme 7. Stannylation of 3-bromo-5-(pyridin-2-ylethynyl)benzonitrile.

.

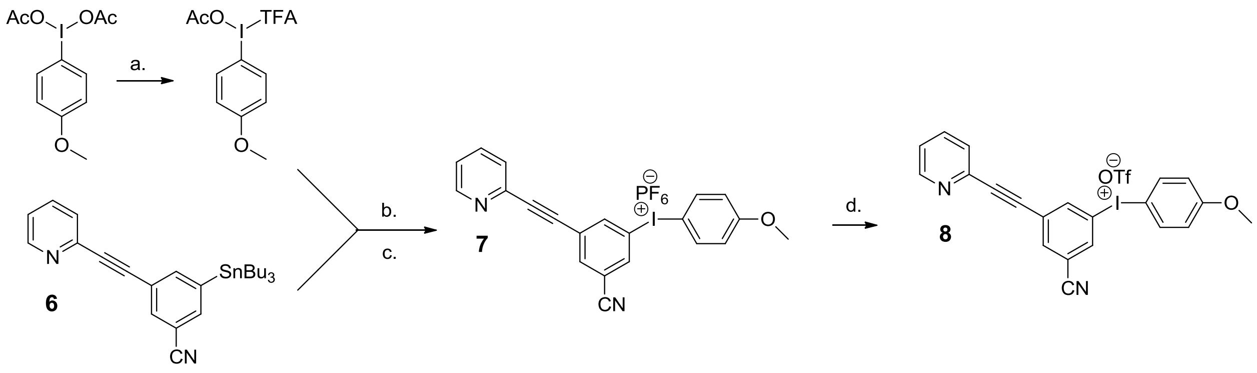

Scheme 8. Iodonium chemistry of PEB. Reagents and conditions: (a)TMS-TFA acetonitrile; (b) CH_3CN, 40 ^oC, 14 hrs. (c) H_2O, $NaPF_6$; (d) Ion-exchange column.

Preparation of the PEB derived diaryliodonium triflate is shown in Scheme 7. The stannane condensed smoothly with 4-methoxyphenyliodonium diacetate upon activation with trifluoroacetic acid (TFA). In this process, TFA replacing once acetate group with a trifluoroacetate, making the I(III) center more electrophilic. Isolation of the diaryliodonium salt was facilitated by the addition of aqueous NaPF6 to precipitate it from water, and extraction with hexane to remove the various tributyl-impurities. Ion-exchange (Amberlite-IRA 400 ion exchange resin) to the triflate was facile.

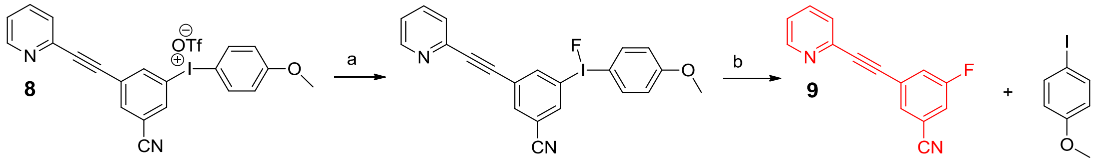

Scheme 9. Fluorination procedure for PEB. A. TMAF, CH_3CN. B. Pumped off CH_3CN, dissolve in C_6H_6, filter and heat to 140 ^oC.

Our laboratory has optimized procedures for thermal decomposition of diaryliodonium salts.[19] It was found that the use of a low polarity, non-coordinating solvents, would improve yields of fluorinated arenes and suppresses noxious side products arising from electron-transfer and disproportionation processes. Prior to this work, the use of benzene as a solvent in PET radiotracer synthesis was unprecedented; the typical solvents are polar aprotic (CH_3CN, DMF). Also, our laboratory has shown that the removal of electrolytes also improves yields significantly. Inorganic salts produced from ion exchange should not act in the thermal decomposition of diaryliodonium salts, but they may act in ligand exchange and increase the I-F dissociation rate and dissociation constant.[19]

To prepare the [^{19}F]-fluorinated PEB derivatives the triflate salt was dissolved in an acetonitrile solution of tertamethyl ammonium fluoride (TMAF). Exchange of triflate and fluoride is instantaneous and verified by ^{19}F NMR spectroscopy. To remove the inert electrolyte (TMA-OTf), the acetonitrile was evaporated and the remainder was dissolved, to the extent possible, in dry d_6-benzene. This solution was passed through a 0.20 um PTFE syringe filter. Reductive elimination of F-PEB was achieved simply by heating the benzene solution at 140 ^oC (sealed tube) for 20 minutes. Fluorination was very selective, no fluoroanisole was formed. The F-PEB was separated from 4-iodoanisole by using a column chromatography (silica gel, ethyl acetate : hexane, 85:15) (70%).

There has been research attention placed on mGluR5 radiotracers that contain a methyl group adjacent to a nitrogen atom in one of the rings.15 PEB was taken as a template, and methyl-Pyridinylethynyl Benzonitrile was investigated as a potential target for this project. As expected the synthetic strategy was high yielding, 60% fluorinated drug; and highly selective, no fluoroanisole formation.

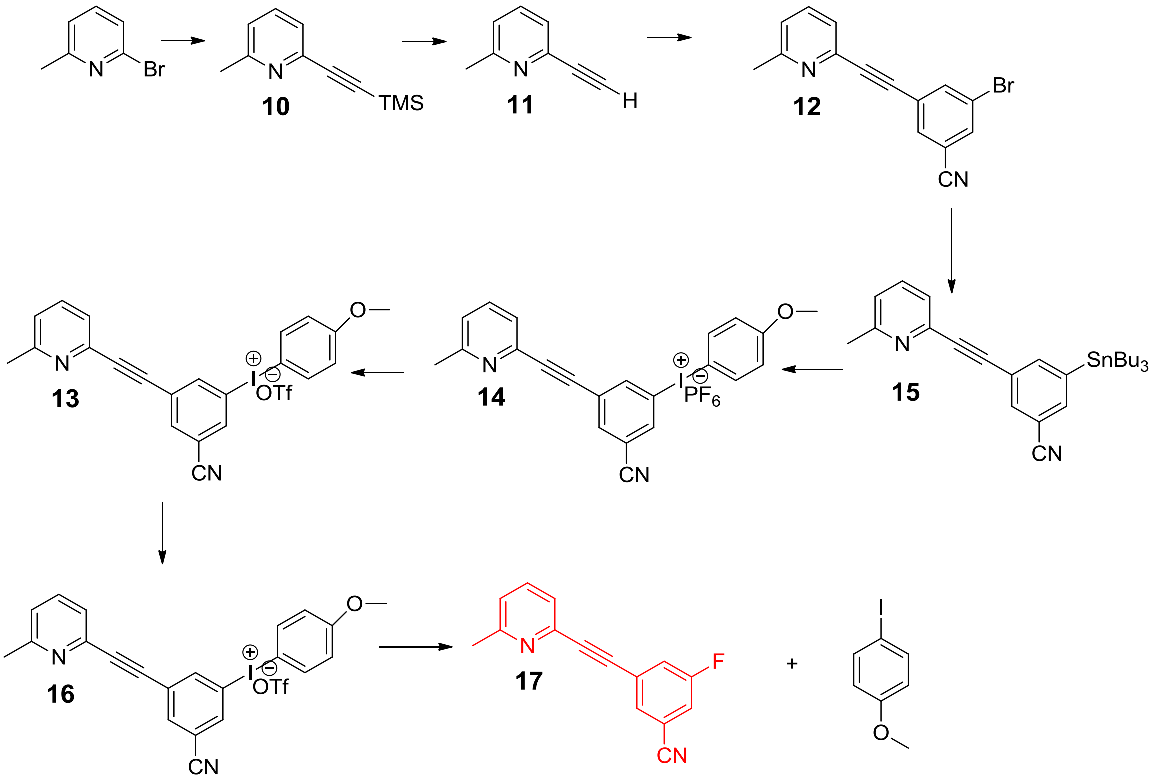

Scheme 10. Synthetic strategy for M-PEB.

The fore mentioned synthesis was performed on methyl-Pyridinylethynyl Benzonitrile, MPEB. All reagents and conditions were exactly the same; detailed characterization can be found in the experimental section.

CHAPTER THREE

3.1 Expansion of Methodology to Aromatic Amino Acids

Glucose (2FDG) has been used in PET imaging to show tumor location. Tumors show an increase of glucose uptake and metabolism, this may is due to the higher energy demands of a rapidly proliferating cell and over expression of glucose transporters. A drawback to using glucose as a PET tracer is that it is not specific, and it would also show up in areas of normal high glucose usage, i.e. the brain and the heart. Many amino acids have been investigated as radiotracers to solve the high background response in 2FDG. R. M. Johnstone in 1965 showed that amino acid transport and protein synthesis is increased in tumor cells.[20] Amino acids can be used as radiotracers, and can be used to visualize amino acid accumulation in tumor tissue; in some cases the amino acid tracers are actually incorporated into growing protein inside tumor cells. Advantages of using amino acids as radiotracers is that they have a higher specificity for particular cancer cells, especially in the brain, and are less likely to give rise to high background signals, as is the case for 2-FDG.[21] Figure 7 shows two very recent fluorinated amino acid radiotracers used in PET imaging.

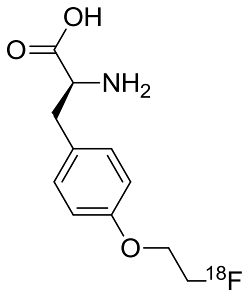

[^{18}F]FET

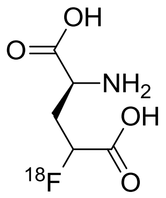

BAY 85-8050

Figure 8. Current amino acid analogues used for PET imaging. FET, [18F]fluoroethyl tyrosine; BAY 85-8050, 4-[^{18}F]Fluoroglutamic Acid.

[^{18}F]fluoroethyl tyrosine, [^{18}F]FET, is currently under investigation for targeting tumor cells in the brain.[22] [^{18}]FET has one major drawback due to the radiotracer being trapped in peripheral tissue, giving rise to a large background signal. To overcome this challenge BAY 85-8050 was developed. [23] This ^{18}F glutamate derivative has been shown to be taken up selectively in lung and colon cancer cell lines.[23] These initial results demonstrates the potential for ^{18}F labeled amino acid radiotracers to be used in oncology imaging.

Although few examples of ^{18}F-labled amino acids as PET imagers are known, Figure 8 shows the variety of aromatic amino acids that can be ^{18}F radio labeled with the techniques developed in the DiMagno laboratory. [18F]-labeled aromatic amino acids present significant challenges for their synthesis with n.c.a. fluoride; protection schemes need to be developed that are compatible with I(III) salt formation and nucleophilic fluorination.

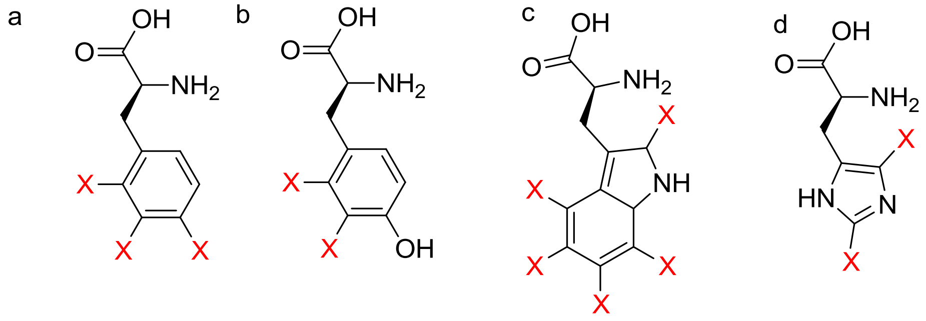

Figure 9. Possible aromatic amino acid radio tracers. Red X implies position of ^{18}F isotope. A. phenylalanine, b. tyrosine, c. tryptophan, d. histidine.

In our approach the position ultimately bearing the ^{18}F-label must be able to be halogenated selectively, and from the halogenated precursor the iodonium chemistry would be identical to the procedure described in Chapter 2.

There is a need to have a high yielding fluorination technique in [^{18}F]-PET. The new method described here, which utilizes iodonium salts, is not only high yielding, but also fits in with the short half-life and fast synthesis that is required for ^{18}F chemistry. This opens the door for usage of ^{18}F labeled drugs in PET imaging.

REFERENCES

1. Cai, L.; Lu, S.; Pike, V. W. European Journal of Organic Chemistry **2008**, 2858-2873.
2. Miller, P. W.; Long, N. J.; Vilar, R.; Gee, A. D. Angew. Chem. Int. Ed **2008**, 47, 8998-9033.
3. Holland, J. P.; Williamson, M. J.; Lewis, J. S. Molecular Imaging **2010**, 9(1) 1-20.
4. DiMagno, S. G.; Sun, H.; Current Topics in Medical Chemistry **2006**, 6, 1473-1482.
5. Global Industry Analyst "Radiopharmaceuticals – A US and European Market Report"
6. Kew, J. N. C.; Kemp, J. A. Psychpharmacology **2005**, 179, 4-29.
7. Nelson, D. L.; Cox, M. M. **200**5. Lehninger: Principles of Biochemistry 4th Ed. New York. W. H. Freeman and Company.
8. Pin, J.P.; Duvoisin, R. Neuropharmacology **1995**, 34(1) 1-26.
9. Gasparini, F.; Bilbe, G.; Gomez-Mancilla, B.; Spooren, W. Current Opinion in Drug Discovery & Development **2008**, 11(5), 655-665. Belanger, M.; Krause, S. M.; Ryan, C.; Sanabria-Bohorquez, S.; Li, W.; Hamill, T.G.; Burns, H. D. Nuclear Medicine Communications **2008**, 29, 915-919.
10. Wang, J.; Brownell, A. Current Medical Imaging Reviews **2007**, 3, 186-205.
11. Schoepp, D. D.; Goldsworthy, J.;Johnson, B. G.;Salhoff, C.R.; Baker, S. R.; Journal of Neurochemistry **1994**, 63(2), 769-772.
12. Varney, M.A; Cosford, N.D.P.; Jachec, C.; Rao, S. P.; Sacaan, A.; Lin, F.; Bleicher, L.; Santori, E. M.; Flor, P.J.; Allgeier, H.; Gasparini, F.; Kuhn, R.; Hess,

S.D.; Velicelebi, G.; Johnson, E.C. Journal of Pharmacology and Experimental Therapeutics **1999**, 290(1), 170-181.

13. Hamill, Terence G.; Krause, Stephen; Ryan, Christine; Bonnefous, Celine; Govek, Steve; Seiders, T. Jon; Cosford, Nicholas D. P.; Roppe, Jeffrey; Kamenecka, Ted; Patel, Shil Synapse **2005**, 56(4), 205-216.
14. Patel, S.; Hamill, T.G.; Connolly, B.; Jagoda, E.; Li, W.; Gibson, R.E. Nuclear Medicine and Biology **2007**, 34, 1009-1017.
15. Alagille, D.; Baldwin, R. M.; Roth, B.L.; Wroblewski, J.T.; Grajkowska, E.; Tamagnan, G.D. Bioorganic & Medicinal Chemistry **2005** , 13, 197-209.
16. Watson, D.A.; Su, M.; Teverovskiy, G.; Zhang, Y.; Garcia-Fortanet, J.; Kinzel, T.; Buchwald, S.L. Science **2009**, 325, 1661-1664.
17. Namavari, M.; Bishop, A.; Satyamurthy, N.; Bida, G.; Barrio, J.R. Applied Radiation and Isotopes **1992**, 43(8), 989-996.
18. Merritt, E.A.; Olofsson, B. Angew. Chem. Int. Ed. **2009**, 48, 9052-9070.
19. Wang, B.; Qin, L.; Neumann, K.D.; Uppaluri, S.; Cerny, R.L.; DiMagno, S.G. Organic Letters **2010**, 12(15), 3352-3355.
20. Johnstone, R.M.; Scholefield, P.G. Adv. Cancer Res. **1965**, 9, 143-226.
21. Kubota, K.; Yamada,K.; Yoshioka, S.; Ito, M.; Ido, T. Clinical Nuclear Medicine **1992**, 17, 361-363.
22. Hess, E.; Sichler, S.; Kluge, A.; Coenen, H.H. Applied Radiation and Isotopes **2002**, 57(2), 185-191.
23. Krasikova, R.N.; Kuznetsova, O.F.; Fedorova, O.S; Belokon, Y.N.; Maleev, V.I. Mu, L.; Ametamev, S.; Schubiger, P.A.; Friebe, M.; Berndt, M.; Koglin, N.;

Mueller, A.; Graham, K.; Lehmann, L.; Dinkelborg, L.M. Journal of Medicinal Chemistry **2011**, 54, 406-410.

EXPERIMENTAL PROCEDURES

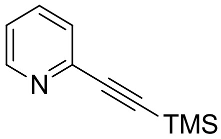

2-((trimethylsilyl)ethynyl)pyridine

Ref: Bioorg. Med. Chem. Let. 16 (2006) 4788-4791

Into a 50 mL schlenk tube was placed triethylamine (15 mL), 2-bromopyridine (2.0g, 12.66 mmol), and trimethylsilylacetylene (1.65 mL, 15.12 mmol). The reaction mixture was freeze, pumped, thawed three times. The reaction mixture was transferred to a small storage tube charged with $Pd(PPh_3)_2Cl_2$ (0.145g, 5 mol %), CuI (0.0049 g, 5 mol %), and a flea stir bar. The solution was capped and heated to 90 ^oC for 12 hrs. Once the reaction was completed the storage tube was cooled to room temperature and contents run through a silica plug with ethyl acetate, to remove the catalyst. The elutant was concentrated via rotary evaporation. The concentrate was purified by flash chromatography (silica gel, 95 : 5 hexanes : ethyl acetate elutant). The solvent was removed in vacuo leaving the product as a brown oil. (2.1 g, 95%)

^1H NMR (400 MHz, $CDCl_3$): δ = 8.5 (dd, 1 H, J_1 = 0.4 Hz, J_2 = 4.8 Hz), 7.71 (dt, 1 H, J_1 = 1.6 Hz, J_2 = 7.8 Hz), 7.4 (td, 1 H, J_1 = 0.8 Hz, J_2 = 7.8 Hz), 7.3 (ddd, 1 H, J_1 = 4.8, J_2 = 3.6, J_3 = 7.8), 0.25 (s, 3 H). ^{13}C NMR (100 MHz, CD_3CN): δ = 151.1, 143.63, 137.46, 128.29, 124.47, 118.29, 105.12, 94.72, -0.25.

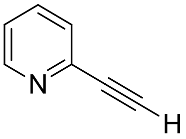

2-((trimethylsilyl)ethynyl)pyridine

In a 100 mL round bottom flask was placed methanol (20 mL), KOH (0.18g, 3.2 mmol), and 2 trimethylsilylethynyl pyridine (300 mg, 1.7 mmol). Solution was allowed to stir at room temperature for 2 hrs. The solvent was removed in vacuo. Concentrate was combined with 10 mL of water. Product was extracted with three washes of ethyl acetate. Product was dried over sodium sulfate and solvent was removed via rotary evaporation yielding a light yellow oil. No further purification was necessary. (0.176g, 100 %)

^{1}H NMR (400 MHz, $CDCl_3$): δ = 8.55(d, 1 H, J = 4.8 Hz), 7.62 (dt, 1 H, J_1 = 6.4 Hz, J_2 = 1.6 Hz), 7.44 (d, 1 H, J = 8Hz), 7.22 (t, 1 H, J = 5.6 Hz), 3.13 (s, 1 H). ^{13}C NMR (100 MHz, $CDCl_3$) : δ = 150.02, 142.32, 136.16, 127.45, 123.41, 82.73, 77.14.

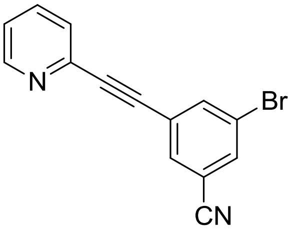

3-bromo-5-(pyridin-2-ylethynyl)benzonitrile

Into a schlenk tube was placed dibromobenzonitrile (4.0 g, 15.7 mmol), 2-ethynyl pyridine (1.84 g, 15.7 mmol), and triethylamine (~50 mL). Reaction mixture was degassed by freeze, pump, thawing three times. Solution was transferred to a storage tube containing $Pd(PPh_3)_2Cl_2$ (0.375 g, 3 mol %), and a catalytic amount of CuI. Storage tube was capped and heated to 90 °C for 18 hrs. Once the reaction was completed the storage tube was cooled to room temperature and contents run through a silica plug with ethyl acetate, to remove the catalyst. The solvent was concentrated via rotary evaporation. The concentrate was purified by flash chromatography (silica gel, 80 : 20 hexanes : ethyl acetate). The solvent was removed in vacuo leaving the product was an off white solid (1.99, 45 %).

^{1}H NMR (400 MHz, $CDCl_3$): δ = 8.6 (dd, 1 H, J_1 = 1.4 Hz, J_2 = 2.8 Hz), 7.9 (t, 1 H, J = 1.6 Hz), 7.8 (dt, 1 H, J_1 = 1.6 Hz, J_2 = 7.6), 7.7 (td, 1 H, J_1 = 1.6 Hz, J_2 = 7.6 Hz), 7.5 (d, 1 H, J = 8 Hz), 7.3 (ddd, 1 H, J_1 = 1.2 Hz, J_2 = 3.6 Hz, J_3 = 7.6 Hz). ^{13}C NMR (100 MHz, $CDCl_3$): δ = 150.36, 142.08, 138.83, 136.41, 134.62, 133.71, 127.54, 125.61, 123.74, 122.85, 116.54, 114.42. 91.95, 84.80.

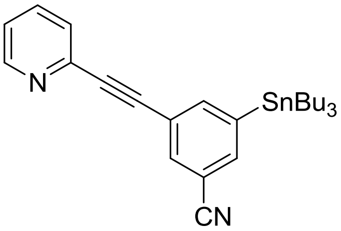

3-(Pyridin-2-ylethynyl)-5-(tributylstannyl)benzonitrile

3-Bromo-5-(pyridin-2-ylethynyl) benzonitrile (0.500g, 1.77 mmol) was dissolved in a minimal amount of benzene and transferred to a heavy-walled glass storage tube equipped with a threaded PTFE closure. Hexabutylditin (3.07g, 5.30 mmol), and benzene

(10 mL) were added. Bis(tri-tert-butylphosphine)palladium was prepared as follows: Pd(dba)$_2$ (80.8 mg, 0.0883 mmol) and P(t-Bu)$_3$ (44.6 mg, 0.221 mmol) were dissolved separately in benzene and combined. The catalyst mixture was allowed to stir until the solution changed from deep purple to dark red, and the solution was passed through a 0.2 μm membrane filter and added directly to the storage tube. The reaction flask was sealed, protected from light by shielding with aluminum foil, and the solution was heated at 110 °C for 3 days. The solution was cooled, the benzene was removed in vacuo, and the crude product was purified by flash chromatography (silica gel, 93:7 hexanes:triethylamine eluant). The solvent was removed in vacuo leaving the product as a viscous yellow oil (0.350g**,** 40%).

^{1}H NMR (300 MHz, CD$_3$CN): δ = 8.4 (d, 1 H, J = 4.2 Hz), 7.87 (s, 1 H), 7.56 (s, 1 H), 7.29 (d, 1 H, J = 1.8 Hz), 7.20 (s, 1 H), 6.88 (dt, 1 H, J$_1$ = 2.0 Hz, J$_2$ = 1.9 Hz), 6.50 (dd, 1 H, J$_1$ = 5.0 Hz, J$_2$ = 7.8 Hz), 1.542 (t, 1 H, J = 8.0 Hz), 1.31 (q, 6 H, J = 16 Hz), 1.15 (h, 6 H, J = 8.2 Hz), 0.884 (t, 9 H, J = 7.2 Hz). ^{13}C NMR (75 MHz, CD$_3$CN): δ = 150.4, 142.8, 139.0, 135.4, 129.9, 127.7, 127.0, 123.4, 122.7, 118.3, 113.2, 29.0, 27.3, 13.6, 9.6. HR-FAB MS: $(M+H)^+$ = 495.1831 m/z (calcd for $C_{26}H_{34}N_2Sn$, 494.174)

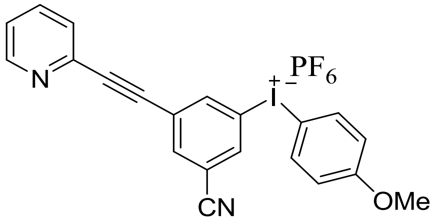

(3-Cyano-5-(pyridine-2-ylethynyl)phenyl)(4-methoxyphenyl)iodonium hexafluorophosphate

3-(Pyridin-2-ylethynyl)-5-(tributylstannyl)benzonitrile (25.0 mg, 0.0500 mmol), 4-methoxyphenyliodonium diacetate (35.8mg, 0.0999 mmol), and trimethylsilyl trifluoroacetate (20.5mg, 0.110 mmol) were combined in CD_3CN and placed in a J. Young NMR tube. The reaction mixture was heated at 40 °C for 11 h, and its progress was monitored by ^1H NMR spectroscopy. Upon completion of the reaction, water (4.5 mL) was added to precipitate tributyltin acetate and the solution was filtered. Sodium hexafluorophosphate (25.19 mg, 0.150 mmol) was added to the filtrate and the precipitated (3-cyano-5-(pyridine-2-ylethynyl)phenyl)(4-methoxyphenyl)iodonium hexafluorophosphate was collected by membrane filtration. The solid was redissolved in CH_2Cl_2 to remove it from the filter and the solvent was evaporated. The colorless solid was recrystallized from CH_2Cl_2/heptanes to give a colorless, crystalline solid. (14.6 mg**,** 50%).

^1H NMR (300 MHz, CD_3CN) δ = 8.63 (d, 1 H, J = 4.8 Hz), 8.49 (d, 1 H, J = 1.2 Hz), 8.40 (s, 1 H), 8.21 (d, 1 H , J = 0.8 Hz), 8.01 (d, 2 H, J = 9.2 Hz), 7.90 (t, 1 H, J = 7.6 Hz), 7.68 (d, 1 H, J = 7.6 Hz), 7.48 (t, 1 H, J = 6.2 Hz), 7.10 (d, 2 H, J = 9.2 Hz), 3.86 (s, 3 H); ^{13}C NMR (75 MHz, CD3CN) d = 150.51, 141.36, 139.12, 138.22, 137.92, 136.81, 127.89, 124.35, 118.44, 117.30, 115.64, 55.84; ^{19}F NMR (282 MHz, CD_3CN): -72.96 (d, 6 F, J = 705 Hz); HR-FAB MS: $(M-PF_6)^+$ 437.0149 m/z (calcd for $C_{21}H_{14}IN_2O$, 437.0145)

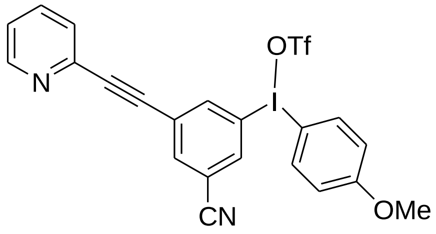

(3-Cyano-5-(pyridine-2-ylethynyl)phenyl)(4-methoxyphenyl)iodonium trifluoromethanesulfonate

(3-cyano-5-(pyridine-2-ylethynyl)phenyl)(4-methoxyphenyl)iodonium hexafluorophosphate (52mg, 0.0894 mmol) was dissolved in a minimal amount **(**0.5mL**)** of acetonitrile. The solution was passed through a 12 mm diameter column packed to a height of 10 cm with Amberlite-IRA 400 ion exchange resin (OTf) in acetonitrile. Evaporation of the eluted product yielded a colorless solid that was recrystallized from acetone/hexane to yield (3-cyano-5-(pyridine-2-ylethynyl)phenyl)(4-methoxyphenyl)iodonium trifluoromethanesulfonate (52.0 mg, 100%)

^{1}H NMR (300 MHz, CD_3CN) δ = 8.64 (d, 1 H, J = 7.0 Hz), 8.47 (s, 1 H), 8.39 (s, 1 H), 8.20 (s, 1 H), 8.06 (d, 2 H, J = 9.3 Hz), 7.82 (d, 1 H, J = 7.5 Hz), 7.63 (d, 1 H, J = 8.4 Hz), 7.40 (d, 1 H, J = 7.0 Hz), 7.09 (d, 2 H, J = 9.0 Hz), 3.86 (s, 3 H); ^{13}C NMR (75 MHz, CD_3CN): 163.79, 159.71, 141.49, 139.30, 138.29, 138.22, 118.46, 116.54, 113.15, 81.87, 55.85, 55.04; ^{19}F NMR (282 MHz, CD_3CN): -79.35 (s); HR-FAB MS: $(M\text{-}OTf)^+$ 437.0156 m/z (calcd for $C_{21}H_{14}IN_2O$, 437.0145)

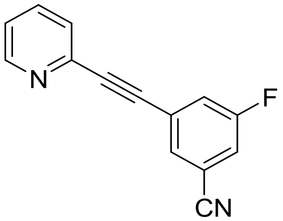

3-Fluoro-5-(pyridine-2-ylethynyl)benzonitrile

(3-Cyano-5-(pyridine-2-ylethynyl)phenyl)(4-methoxyphenyl)iodonium trifluoromethanesulfonate (25 mg, 0.0427 mmol) and TMAF (3.3mg, 0.0417 mmol) were combined in CH_3CN to effect ion exchange. The solvent was removed in vacuo, the residue was treated with C_6D_6 (0.8 mL) and the solution was passed through a membrane filter (0.2 μm pore size) directly into an NMR tube that was equipped with a PTFE valve. The reaction mixture was heated at 140 ºC for 15 minutes. Product was purified by flash chromatography (silica gel, 85:15 hexanes:ethyl acetate eluant). The solvent was removed in vacuo leaving the product as a crystalline white powder (7 mg, 70%)

^{19}F NMR (376 MHz, CD_3CN): -111.81 (t)

Preparation of an analytical standard of 3-Fluoro-5-(pyridine-2-ylethynyl)benzonitrile

A sample of 3-fluoro-5-(pyridine-2-ylethynyl)benzonitrile was performed by standard methods to provide an analytical HPLC standard. 2-Ethynylpyridine (100 mg, 0.971 mmol) and 2-bromo-4-fluorobenzonitile (192 mg, 0.965 mmol) were dissolved separately in trimethylamine (5 mL) and placed into a heavy-walled glass storage tube equipped with a threaded PTFE closure. The reaction mixture was degassed and transferred by cannula into a separate heavy-walled glass storage tube fitted with a threaded PTFE closure containing bis(triphenylphosphine)palladium dichloride (34 mg, 5 mol %) and CuI (4.3 mg, 5 mol %). The reaction was capped and heated to 80 °C for 18 h. The cooled solution was extracted from water using ethyl acetate, and the organic layer was dried over sodium sulfate. Flash chromatography (silica gel, 95:5 hexanes:ethyl acetate eluant) and evaporation of the solvent provided the product as a light yellow solid. Recrystallization was performed with hexanes to yield colorless crystals. (64.7 mg, 30 %)

^{1}H NMR (400 MHz, CD_3CN): $\delta = 8.62$ (dd, 1 H, $J_1 = 0.8$ Hz, $J_2 = 3.4$ Hz), 7.81 (dt, 2 H, J_1=2.0 Hz, J_2= 7.8 Hz), 7.66 (ddd, 1 H, $J_1 = 1.6$ Hz, $J_2 = 2.6$ Hz, $J_3 = 9.2$ Hz), 7.62 (td, 1 H, $J_1 = 0.8$ Hz, $J_2 = 8.0$ Hz), 7.59 (ddd, 1 H, $J_1 = 1.2$ Hz, $J_2 = 2.4$ Hz, $J_3 = 8.4$ Hz), 7.39 (ddd, 1 H, $J_1 = 0.8$ Hz, $J_2 = 5.0$ Hz, $J_3 = 8.0$ Hz); ^{13}C NMR (75 MHz, CD_3CN): $\delta = 168.87$, 165.58, 155.70, 147.25, 141.99, 137.15, 137.10, 133.96, 130.96, 130.82, 129.29, 128.83, 128.52, 125.43, 125.10, 119.65, 119.51, 96.57; ^{19}F NMR (376 MHz, CD_3CN): -111.81 (t, 1 F); HR-FAB MS: $(M+H)^+$ = 223.0674 (calcd for $C_{14}H_7FN_2$, 222.06)

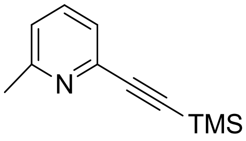

2-methyl-6-((trimethylsilyl)ethynyl)pyridine

Into a 50 mL schlenk tube was placed triethylamine (30 mL), 2-bromo-6-methylpyridine (2.0g, 11.63 mmol), and trimethylsilylacetylene (1.36 mL, 13.95 mmol). The reaction mixture was freeze, pumped, thawed three times. The reaction mixture was transferred to a small storage tube charged with $Pd(PPh_3)_2Cl_2$ (0.163 g, 2 mol %), CuI (0.044 g, 2 mol %), and a flea stir bar. The solution was capped and heated to 90 oC for 12 hrs. Once the reaction was completed the storage tube was cooled to room temperature and contents run through a silica plug with ethyl acetate, to remove the catalyst. The elutant was concentrated via rotary evaporation. The concentrate was purified by flash chromatography (silica gel, 95 : 5 hexanes : ethyl acetate elutant). The solvent was removed in vacuo leaving the product as a brown oil. (2.09 g, 95 %)

^{1}H NMR (400 MHz, $CDCl_3$): δ = 7.5 (t, 1 H, J1 = 7.6 Hz), 7.2 (d, 1 H, 7.6 Hz), 7.0 (d, 1 H, 7.6 Hz), 2.5 (s, 3 H), 0.2 (s, 9 H). ^{13}C NMR (100 MHz, $CDCl_3$): δ = 158.84, 142.31, 136.25, 124.57, 122.85, 103.88, 94.16, 24.57, -0.24.

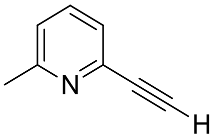

2-methyl-6-((trimethylsilyl)ethynyl)pyridine

In a 100 mL round bottom flask was placed methanol (33 mL), KOH (1.29g, 23.0 mmol), and 2 trimethylsilylethynyl pyridine (2.09 g, 17.9 mmol). Solution was allowed to stir at room temperature for 2 hrs. The solvent was removed in vacuo. Concentrate was combined with 10 mL of water. Product was extracted with three washes of ethyl acetate. Product was dried over sodium sulfate and solvent was removed via rotary evaporation yielding a light yellow oil. No further purification as necessary. (1.19g, 92 %).

^{1}H NMR (300 MHz, $CDCl_3$): δ = 7.56 (t, 1 H, J = 7.8 Hz), 7.32 (d, 1 H, J = 7.5), 7.15 (d, 1 H, J = 7.8), 3.14 (s, 1 H), 2.57 (s, 3 H).

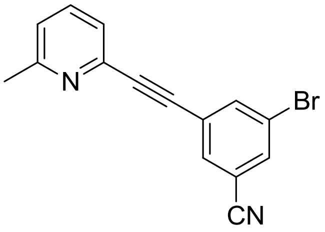

3-bromo-5-((6-methylpyridin-2-yl)ethynyl)benzonitrile

Into a schlenk tube was placed dibromobenzonitrile (3.15g,12.2 mmol), 2-ethynyl-6-methyl pyridine (1.19g, 10.17 mmol), and triethylamine (~50 mL). Reaction mixture was degassed by freeze, pump, thawing three times. Solution was transferred to a storage tube containing $Pd(PPh_3)_2Cl_2$ (3 mol %), and a catalytic amount of CuI. Storage tube was capped and heated to 90 C for 18 hrs. Once the reaction was completed the storage tube was cooled to room temperature and contents run through a silica plug with ethyl acetate, to remove the catalyst. The solvent was concentrated via rotary evaporation. The concentrate was purified by flash chromatography (silica gel, 85 : 15 hexanes : ethyl acetate). The solvent was removed in vacuo leaving the product was an off white solid (1.78g, 59%).

^1H NMR (400 MHz, $CDCl_3$): δ = 7.66 (s, 1 H), 7.6 (t, 1 H, J = 8 Hz), 7.5 (dq, 1 H, J_1 = 8.8 Hz, J_2 = 1.6 Hz), 7.36 (d, 1 H, J = 8 Hz), 7.35 (dq, 1 H, J_1 = 12 Hz, J_2 = 1.2 Hz), 7.1 (d, 1 H, J = 7.6 Hz), 2.6 (s, 3 H). ^{13}C NMR (100 MHz, $CDCl_3$): δ = 163.08, 160.59, 159.29, 141.28, 136.56, 131.39, 126.22, 124.83, 123.35, 119.38, 116.79, 114.39, 92.03, 84.54, 24.66.

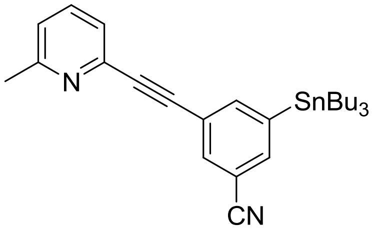

3-((6-methylpyridin-2-yl)ethynyl)-5-(tributylstannyl)benzonitrile

3-bromo-5-((methylpyridin-2-yl) ethynyl) benzonitrile (1g, 1.97 mmol) was dissolved in a minimal amount of benzene and transferred to a heavy walled glass storage tube equipped with a threaded PTFE closure. Hexabutylditin (3.44g, 5.90 mmol), and benzene (10ml) were added. Bis(tri-tert-butylphosphine) palladium was prepared as follows: Pd(dba)$_2$ (0.126 mg, 0.138 mmol) and P(t-Bu)$_3$ (69.8 mg, 0.345 mmol) were dissolved separately in benzene and combined. The catalyst mixture was allowed to stir until the solution changed from a deep purple to a dark red. The catalyst mixture was passed through a 0.2 um membrane filter and directly to the storage tube. The reaction flask was sealed, protected from light by shielding with aluminum foil, and the solution was heated to 110 ^{o} C for 3 days. The solution was cooled, the benzene was removed in vacuo, and the crude product was purified by flash chromatography (silica gel, 90:10 hexanes:triethylamine eluant). The solvent was removed in vacuo leaving the product as a viscous yellow oil (0.460 g, 46%).

^{1}H NMR (400MHz, CD$_3$CN): δ = 7.93 (d, 1 H, J = 0.8 Hz), 7.84 (s, 1 H), 7.83 (s, 1 H), 7.67 (t, 1 H, J = 7.8 Hz), 7.41 (d, 1 H, J = 7.6 Hz), 7.24 (d, 1 H, J = 8.0 Hz), 2.51 (s, 3 H), 1.52 (q, 6 H, J = 8.6 Hz), 1.39 (s, 6 H, J = 6.9 Hz), 1.15 (t, 6 H, J = 7.8 Hz), 0.88 (t, 9 H, J = 7.35 Hz); ^{13}C NMR (75 MHz, CD$_3$CN): δ = 159.30, 145.21, 143.31, 141.62, 139.69, 136.82, 134.44, 124.57, 123.22, 122.66, 118.18, 112.18, 90.53, 85.90, 28.66, 26.95, 23.52, 12.92, 9.47; HR-FAB MS: $(M+H)^+$ = 509.1979 (calcd for $C_{27}H_{36}N_2Sn$, 508.19)

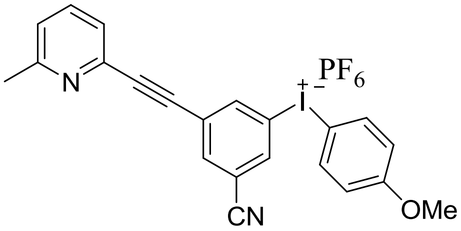

(3-cyano-5-((6-methylpyridin-2-yl)ethynyl)phenyl)(4-methoxyphenyl)iodonium hexafluorophosphate

3-(pyridin-2-ylethynyl-6-methyl)-5-(tributylstannyl)benzonitrile (25.0 mg, 0.0420 mmol), diacetateiodoanisole (29.5mg, 0.0838 mmol), and trimethylsilyl-trifluroacetate (11.7 mg, 0.0630 mmol) were combined in CD3CN and placed in J. Young NMR tube. The reaction mixture was heated to 40 °C for 12 hrs, the reaction was monitored by 1H NMR spectroscopy. Upon completion of the reaction, the reaction mixture was combined with water (4.5g, 0.250 mol) to precipitate the tributyltin-acetate and the solution was filtered. The filtrate was combined with Sodiumhexaflurophosphate (25.19 mg, 0.150 mmol) and the precipitated (3-cyano-5-((6-methylpyridin-2-yl)ethynyl)phenyl)(4-methoxyphenyl)iodonium hexafluorophosphate was collected by membrane filtration. The solid was redissloved in CH2Cl2 to remove it from the filter and the solvent evaporated. The colorless solid was recrystallized from CH2Cl2/heptanes to give a colorless, crystalline solid (12.5mg, 50%).

^{1}H NMR (400MHz, CD_3CN): δ = 8.47 (s, 1 H), 8.39 (s, 1 H), 8.20 (s, 1 H), 8.07 (d, 2 H, J = 8.1 Hz), 7.72 (t, 1 H, J = 8.0 Hz), 7.44 (d, 1 H, J = 8.0 Hz), 7.29 (d, 1 H, J = 8.0 Hz), 7.10 (d, 2 H, J = 9.2 Hz), 3.86 (s, 3 H), 2.52 (s, 3 H). ^{13}C NMR (100 MHz, CD_3CN): δ = 163.82, 159.59, 141.36, 140.57, 139.16, 138.29, 137.89, 137.10, 126.78, 125.09, 124.06, 118.49, 115.66, 112.93, 101.28, 93.33, 82.99, 55.85, 23.46; ^{19}F (376 MHz, CD_3CN) δ = -72.79 (d, 6 F, 703.1 Hz); HR-FAB MS: $(M-PF_6)^+$ 451.0299 m/z (calcd for $C_{22}H_{16}IN_2O$, 451.03)

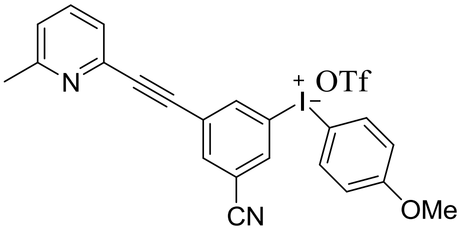

(3-cyano-5-((6-methylpyridin-2-yl)ethynyl)phenyl)(4-methoxyphenyl)iodonium trifluoromethanesulfonate

(3-cyano-5-(pyridine-2-ylethynyl-6-methyl)phenyl)(4-methoxyphenyl)iodonium hexafluorophosphate (50 mg, 0.0839 mmol) was dissolved in a minimal amount(0.5 mL) of acetonitrile. The solution was flowed through a 12 mm diameter column packed to a height of 10 cm with Amberlite-IRA 400 ion exchange resin (OTf) in acetonitrile. Evaporation of the eluted product yielded a colorless solid that was recrystallized from acetone/hexane to yield (3-cyano-5-((6-methylpyridin-2-yl)ethynyl)phenyl)(4-methoxyphenyl)iodonium trifluoromethanesulfonate (50 mg, 100%).

^{1}H NMR (400MHz, CD_3CN): δ = 8.47 (t, 1 H, J = 1.2 Hz), 8.39 (t, 1 H, J = 1.6 Hz), 8.18 (d, 1 H J = 1.2 Hz), 8.07 (dd, 2 H, J_1 = 2.4 Hz, J_2 = 7.2 Hz), 7.70 (t, 1 H, J = 7.8 Hz), 7.44 (d, 1 H, J = 7.6 Hz), 7.29 (d, 1 H, J = 7.6 Hz), 7.09 (dd, 2 H, J_1 = 2.0 Hz, J_2 = 7.2

Hz), 3.82 (s, 3 H), 2.51 (s, 3 H); ^{13}C (75 MHz, CD_3CN): δ = 163.70, 159.60, 141.36, 139.00, 138.24, 137.87, 136.97, 126.70, 125.04, 123.97, 118.38, 115.54, 113.28, 101.66, 55.82, 23.50, 23.50, 0.72; ^{19}F NMR (282 MHz, CD_3CN): δ = -79.30 (s, 3 F); HR-FAB MS: $(M-OTf)^+$ 451.0288 m/z (calcd for $C_{22}H_{16}IN_2O$, 451.03).

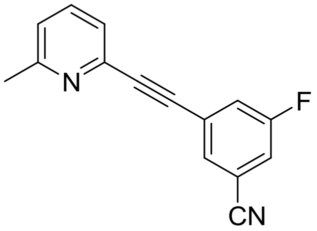

Preparation of an analytical standard of 3- Fluoro-5-(6-methylpyridine-2-ylethynyl)benzonitrile

Preparation of fluorinated standard was done for HPLC analysis. 6-methyl-2-ethynylpyridine (100mg, 0.855 mmol) was placed in a storage tube along with 2-bromo-4-fluorobenzonitile (171 mg, 0.855 mmol) and triethylamine (5 mL). The reactions mixture was degassed and canulated into a storage tube containing Dichloro-ditriphenylphosphine palladium (II) (5 mol%) and CuI (5 mol%). The reaction was capped and heated to 80 °C for 18 hrs. The reaction mixed was removed from heat and an aqueous workup was performed with water and EtOAc. The organic layer was dried over sodium sulfate. Flash chromatography was performed on the reaction mixture, product eluted in 5% triethylamine in hexanes. Product was brown solid. Recrystalization was performed with hexanes to yield white crystals. (30%)

^{1}H(400MHz, CD_3CN): δ = 7.82 (s, 1 H), 7.72 (t, 1 H, J = 7.6 Hz), 7.67 (dd, 1 H, J1 = 1.0 Hz, J2 = 8.2 Hz,), 7.61 (dd, 1 H, J1 = 1.6 Hz, J2 = 8.2 Hz), 7.46 (d, 1 H, J = 7.6 Hz), 7.29 (d, 1 H, J = 8 Hz), 2.54 (s, 3 H); ^{13}C (75 MHz, CD_3CN): δ = 163.56, 160.23, 159.36, 141.24, 136.70, 131.51, 131.47, 126.25, 124.79, 123.65, 123.34, 119.56, 119.23, 116.78, 114.23; ^{19}F (376MHz, CD_3CN): δ = -112.18 (t, 7.52, 1 F); HR-FAB MS: $(M+H)^+$ 237.0825 m/z (calcd $C_{15}H_{10}N_2F$, 236.07)

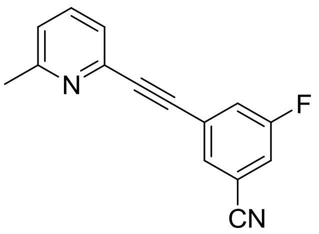

3-fluoro-5-(pyridine-2-ylethynyl-6-methyl)benzonitrile

Triflate precursor (25mg, 0.0427 mmol) was combined with TMAF (3.3mg, 0.0417 mmol) in acetonitrile-d3. This solution is to be kept fairly concentrated, entire process is to be kept air-free. Exchange is instantaneous, and acetonitrile is pumped off. The reaction is redissolved in benzene-d_6, and filtered with a membrane filter. The reaction mixture is heated to 140 ^{o}C for 15 minutes. Product was purified by flash chromatography (silica gel, 85:15 hexanes:ethyl acetate eluant). The solvent was removed in vacuo leaving the product as a crystalline white powder (5.9 mg, 60%).

^{19}F (376MHz, CD_3CN): δ = -112.18 (t, 1 F)

APPENDIX A.

Common Abbreviations Used in this Thesis

PET	Positron Emission Tomography
mGluR	metabotropic glutamate receptor
K. 2.2.2	Krytofix 2.2.2.
RCY	decay-corrected radiochemical yield
PEB	3-Fluoro-5-(pyridine-2-ylethynyl)benzonitrile
CH_3CN	acetonitrile
C_6H_6	benzene
TMAF	Tetramethyl ammonium fluoride
MPEB	3- Fluoro-5-(6-methylpyridine-2-ylethynyl)benzonitrile

APPENDIX B

NMR Spectra

1. ^{1}H of 2-((trimethylsilyl)ethynyl)pyridine in $CDCl_3$
2. ^{13}C of 2-((trimethylsilyl)ethynyl)pyridine in $CDCl_3$
3. ^{1}H of 2-((trimethylsilyl)ethynyl)pyridine in $CDCl_3$
4. ^{13}C of 2-((trimethylsilyl)ethynyl)pyridine in $CDCl_3$
5. ^{1}H of 3-bromo-5-(pyridin-2-ylethynyl)benzonitrile in $CDCl_3$
6. ^{13}C of 3-bromo-5-(pyridin-2-ylethynyl)benzonitrile in $CDCl_3$
7. ^{1}H of 3-(Pyridin-2-ylethynyl)-5-(tributylstannyl)benzonitrile in CD_3CN
8. ^{13}C of 3-(Pyridin-2-ylethynyl)-5-(tributylstannyl)benzonitrile in CD_3CN
9. ^{1}H of (3-Cyano-5-(pyridine-2-ylethynyl)phenyl)(4-methoxyphenyl)iodonium hexafluorophosphate in CD_3CN
10. ^{13}C of (3-Cyano-5-(pyridine-2-ylethynyl)phenyl)(4-methoxyphenyl)iodonium hexafluorophosphate in CD_3CN
11. ^{19}F of (3-Cyano-5-(pyridine-2-ylethynyl)phenyl)(4-methoxyphenyl)iodonium hexafluorophosphate in CD_3CN
12. ^{1}H of (3-Cyano-5-(pyridine-2-ylethynyl)phenyl)(4-methoxyphenyl)iodonium trifluoromethanesulfonate in CD_3CN
13. ^{13}C of (3-Cyano-5-(pyridine-2-ylethynyl)phenyl)(4-methoxyphenyl)iodonium trifluoromethanesulfonate in CD_3CN
14. ^{19}F (3-Cyano-5-(pyridine-2-ylethynyl)phenyl)(4-methoxyphenyl)iodonium trifluoromethanesulfonate in CD_3CN
15. ^{19}F of 3-Fluoro-5-(pyridine-2-ylethynyl)benzonitrile in CD_3CN

16. ^{1}H of 3-Fluoro-5-(pyridine-2-ylethynyl)benzonitrile in CD_3CN

17. ^{13}C of 3-Fluoro-5-(pyridine-2-ylethynyl)benzonitrile in CD_3CN

18. ^{19}F of 3-Fluoro-5-(pyridine-2-ylethynyl)benzonitrile in CD_3CN

19. ^{1}H of 2-methyl-6-((trimethylsilyl)ethynyl)pyridine in $CDCl_3$

20. ^{13}C of 2-methyl-6-((trimethylsilyl)ethynyl)pyridine in $CDCl_3$

21. ^{1}H of 2-methyl-6-((trimethylsilyl)ethynyl)pyridine in $CDCl_3$

22. ^{1}H of 3-bromo-5-((6-methylpyridin-2-yl)ethynyl)benzonitrile in $CDCl_3$

23. ^{13}C of 3-bromo-5-((6-methylpyridin-2-yl)ethynyl)benzonitrile in $CDCl_3$

24. ^{1}H of 3-((6-methylpyridin-2-yl)ethynyl)-5-(tributylstannyl)benzonitrile in CD_3CN

25. ^{13}C of 3-((6-methylpyridin-2-yl)ethynyl)-5-(tributylstannyl)benzonitrile in CD_3CN

26. ^{1}H of (3-cyano-5-((6-methylpyridin-2-yl)ethynyl)phenyl)(4-methoxyphenyl)iodonium hexafluorophosphate in CD_3CN

27. ^{13}C of (3-cyano-5-((6-methylpyridin-2-yl)ethynyl)phenyl)(4-methoxyphenyl)iodonium hexafluorophosphate in CD_3CN

28. ^{19}F of (3-cyano-5-((6-methylpyridin-2-yl)ethynyl)phenyl)(4-methoxyphenyl)iodonium hexafluorophosphate in CD_3CN

29. ^{1}H of (3-cyano-5-((6-methylpyridin-2-yl)ethynyl)phenyl)(4-methoxyphenyl)iodonium trifluoromethanesulfonate in CD_3CN

30. ^{13}C of (3-cyano-5-((6-methylpyridin-2-yl)ethynyl)phenyl)(4-methoxyphenyl)iodonium trifluoromethanesulfonate in CD_3CN

31. ^{19}F of (3-cyano-5-((6-methylpyridin-2-yl)ethynyl)phenyl)(4-methoxyphenyl)iodonium trifluoromethanesulfonate in CD_3CN

32. ^{19}F of 3- Fluoro-5-(6-methylpyridine-2-ylethynyl)benzonitrile in CD_3CN
33. ^{1}H of 3- Fluoro-5-(6-methylpyridine-2-ylethynyl)benzonitrile in CD_3CN
34. ^{13}C of 3- Fluoro-5-(6-methylpyridine-2-ylethynyl)benzonitrile in CD_3CN
35. ^{19}F of 3- Fluoro-5-(6-methylpyridine-2-ylethynyl)benzonitrile in CD_3CN

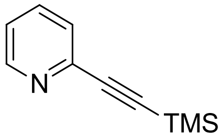
N
TMS

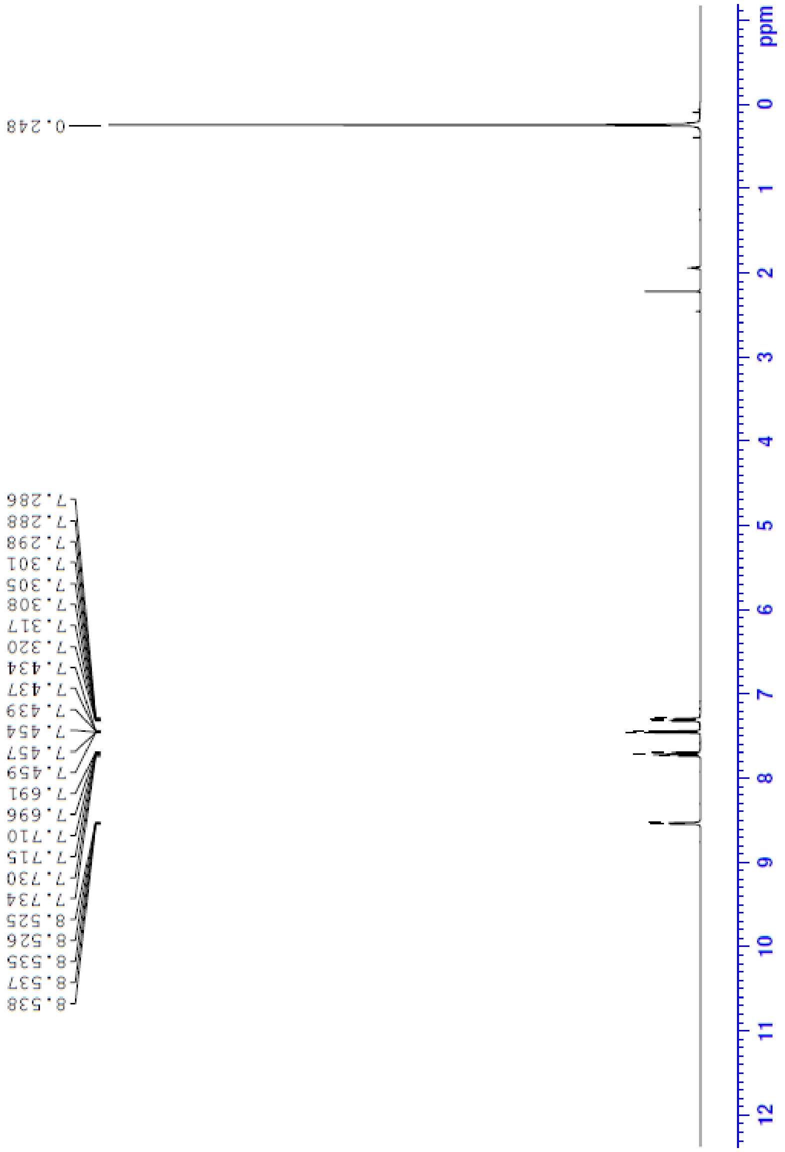
0.248
7.286
7.288
7.298
7.301
7.305
7.308
7.317
7.320
7.434
7.437
7.439
7.454
7.457
7.459
7.691
7.696
7.710
7.715
7.730
7.734
8.525
8.526
8.535
8.537
8.538
ppm
0
1
2
3
4
5
6
7
8
9
10
11
12

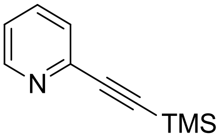
N
TMS

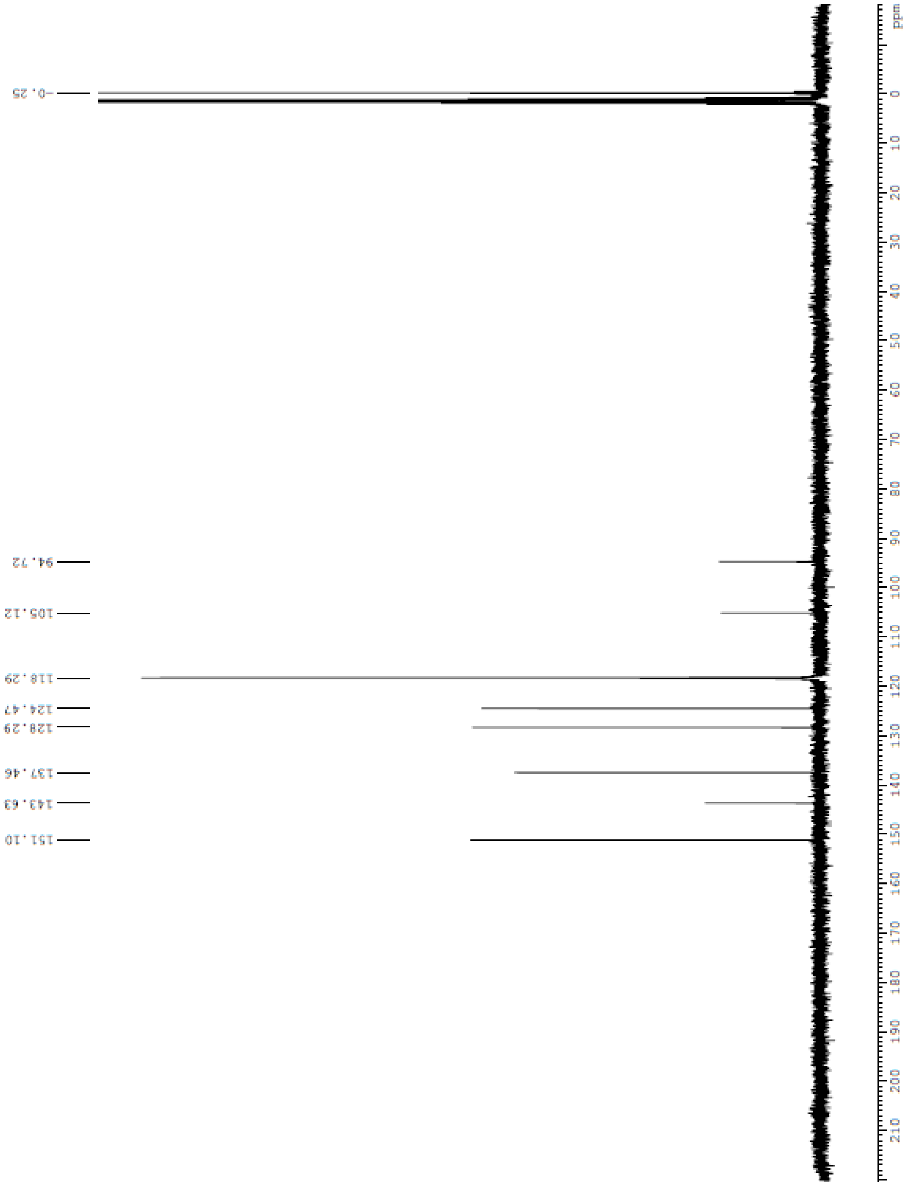
-0.25
94.72
105.12
118.29
124.47
128.29
137.46
143.63
151.10
ppm
0
10
20
30
40
50
60
70
80
90
100
110
120
130
140
150
160
170
180
190
200
210

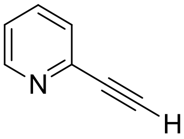
N
H

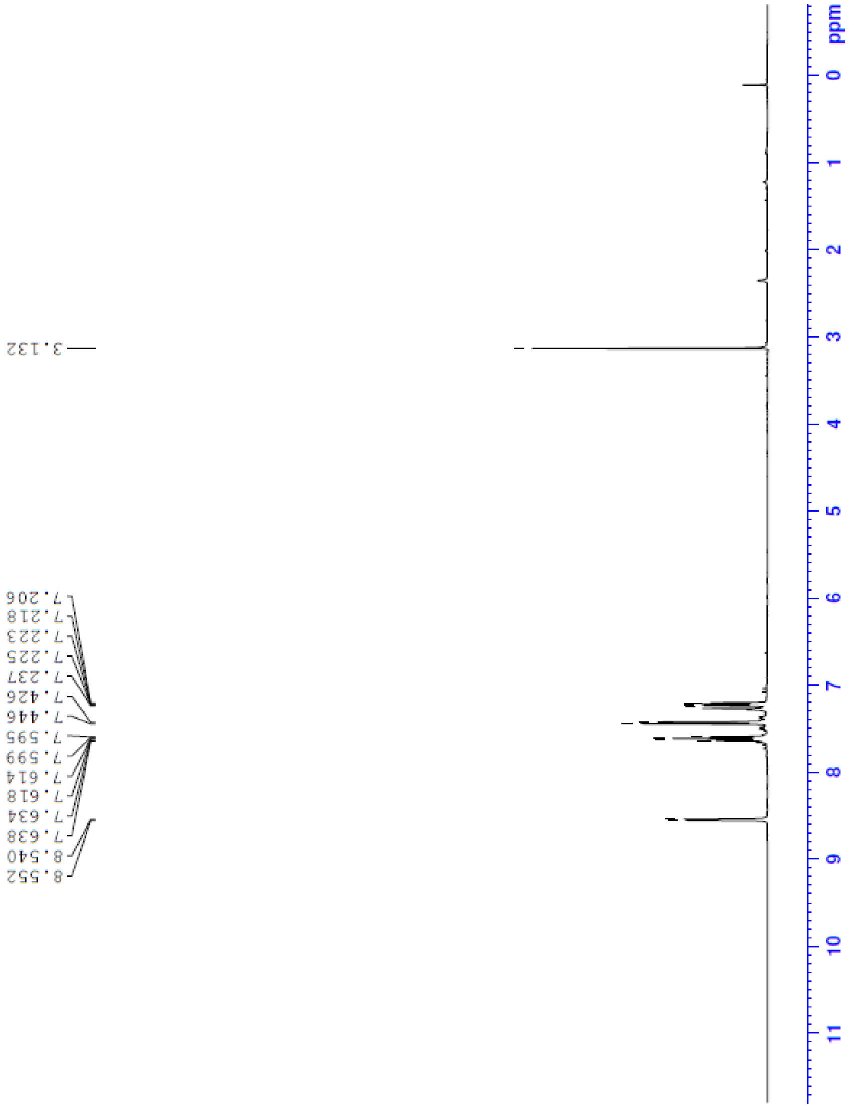
3.132
7.206
7.218
7.223
7.225
7.237
7.426
7.446
7.595
7.599
7.614
7.618
7.634
7.638
8.540
8.552
ppm
0
1
2
3
4
5
6
7
8
9
10
11

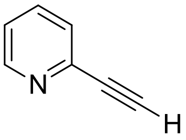
N
H

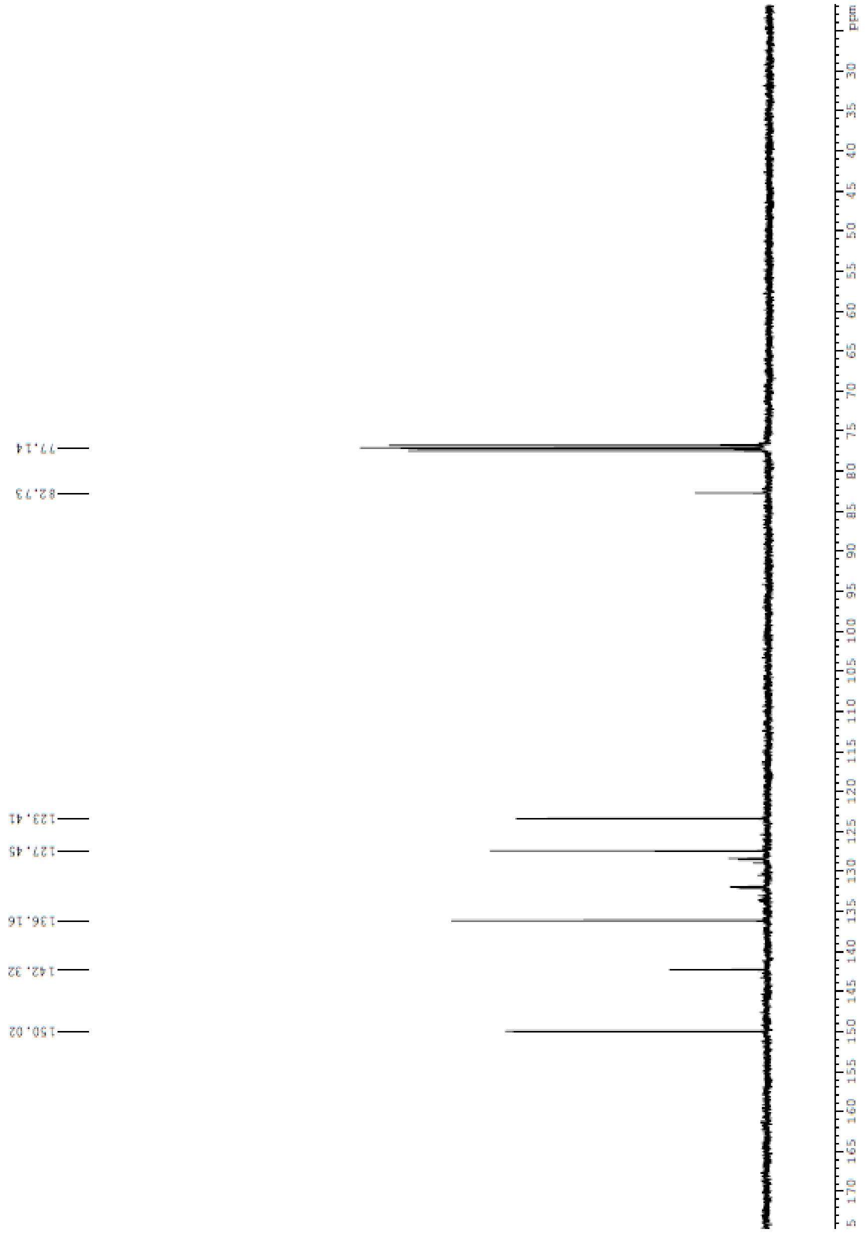
77.14
82.73
123.41
127.45
136.16
142.32
150.02
ppm
30
35
40
45
50
55
60
65
70
75
80
85
90
95
100
105
110
115
120
125
130
135
140
145
150
155
160
165
170

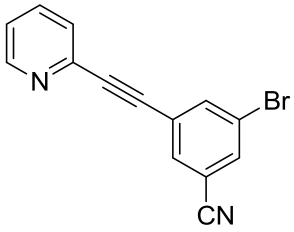
N
Br
CN

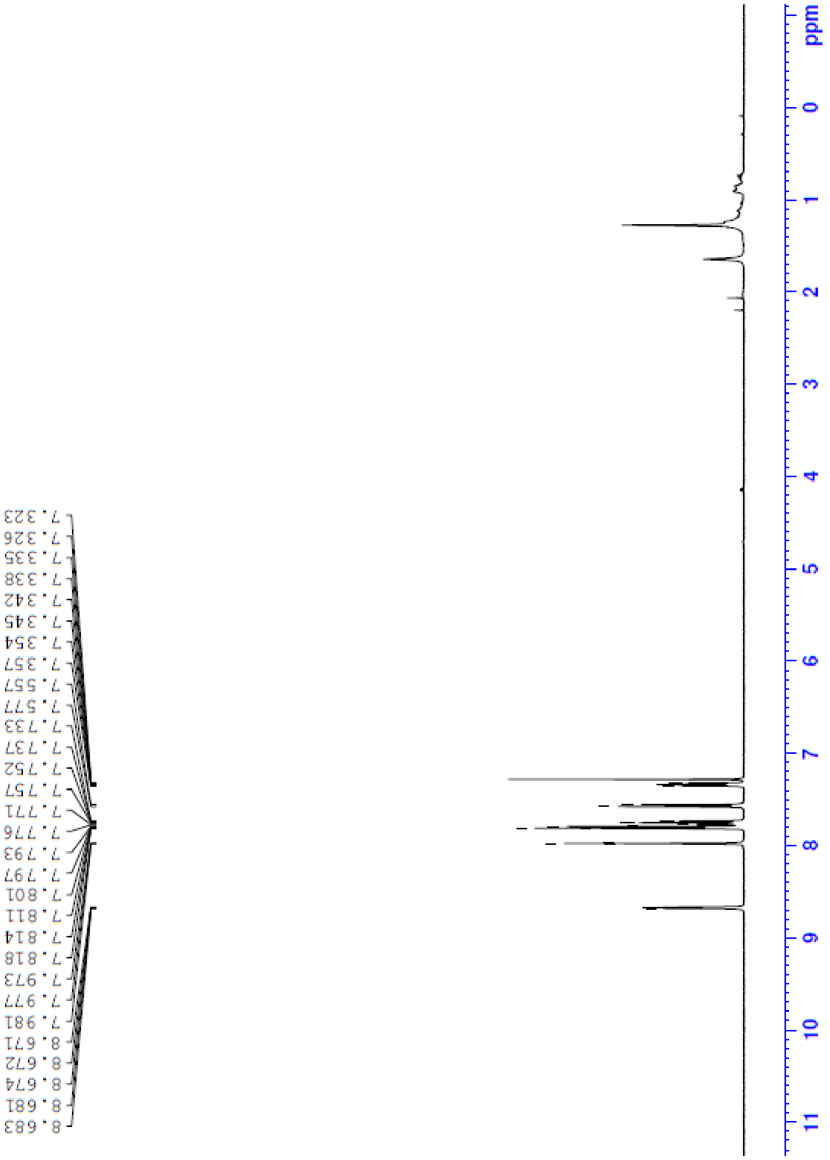
7.323
7.326
7.335
7.338
7.342
7.345
7.354
7.357
7.557
7.577
7.733
7.737
7.752
7.757
7.771
7.776
7.793
7.797
7.801
7.811
7.814
7.818
7.973
7.977
7.981
8.671
8.672
8.674
8.681
8.683
ppm
0
1
2
3
4
5
6
7
8
9
10
11

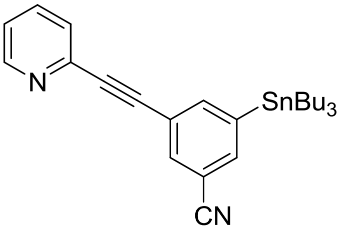
N
SnBu$_3$
CN

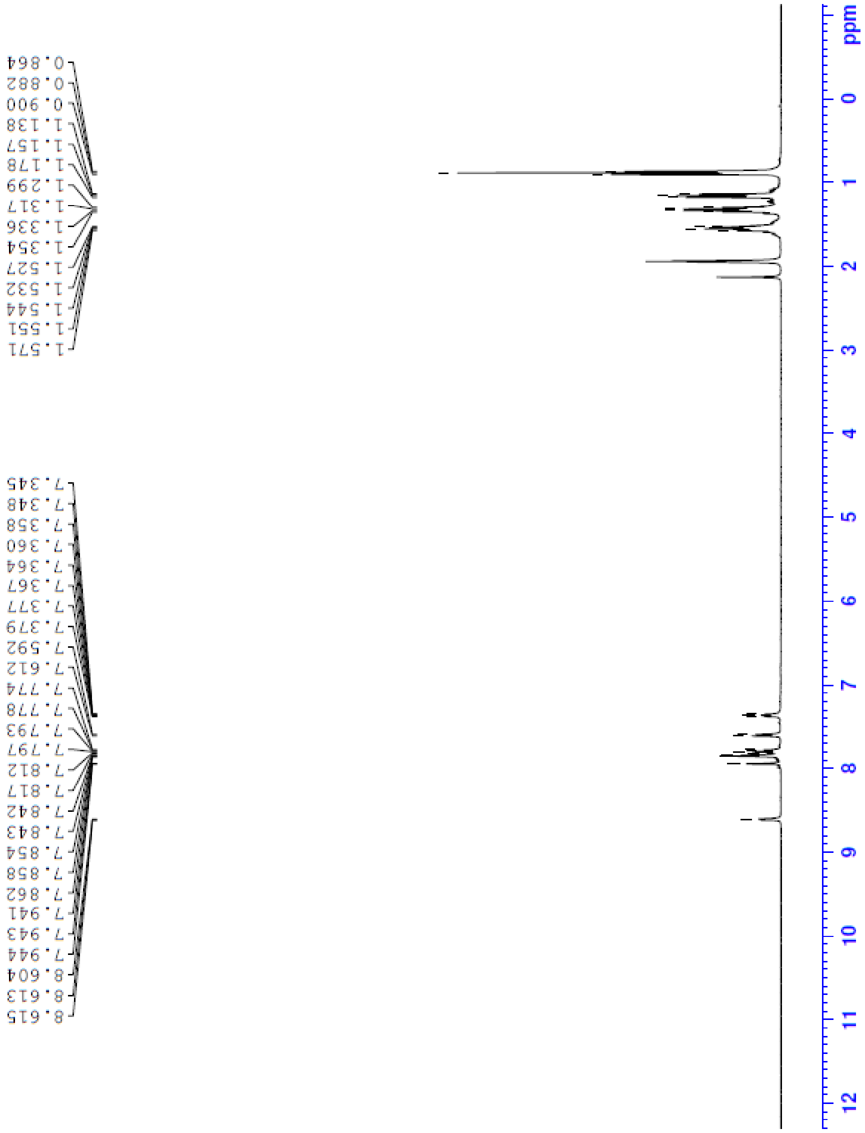
0.864
0.882
0.900
1.138
1.157
1.178
1.299
1.317
1.336
1.354
1.527
1.532
1.544
1.551
1.571
7.345
7.348
7.358
7.360
7.364
7.367
7.377
7.379
7.592
7.612
7.774
7.778
7.793
7.797
7.812
7.817
7.842
7.843
7.854
7.858
7.862
7.941
7.943
7.944
8.604
8.613
8.615
ppm
0
1
2
3
4
5
6
7
8
9
10
11
12

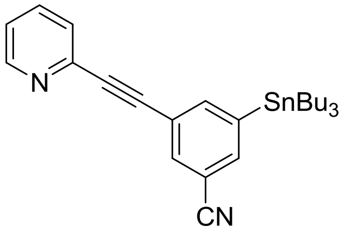
N
SnBu$_3$
CN

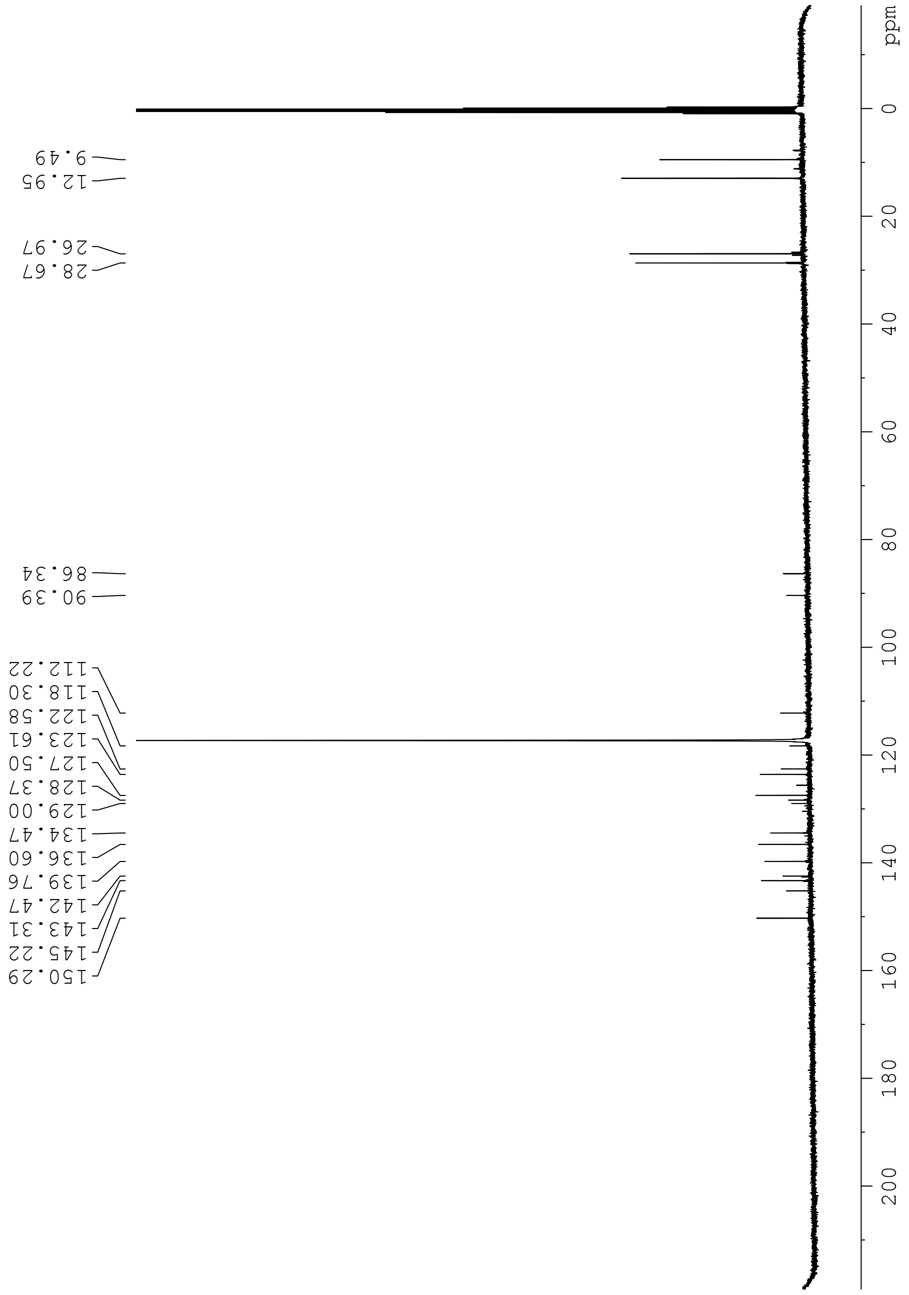
9.49
12.95
26.97
28.67
86.34
90.39
112.22
118.30
122.58
123.61
127.50
128.37
129.00
134.47
136.60
139.76
142.47
143.31
145.22
150.29
ppm
0
20
40
60
80
100
120
140
160
180
200

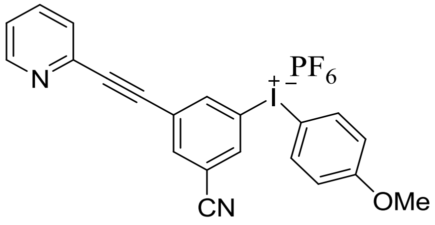
PF6
I
CN
OMe
N

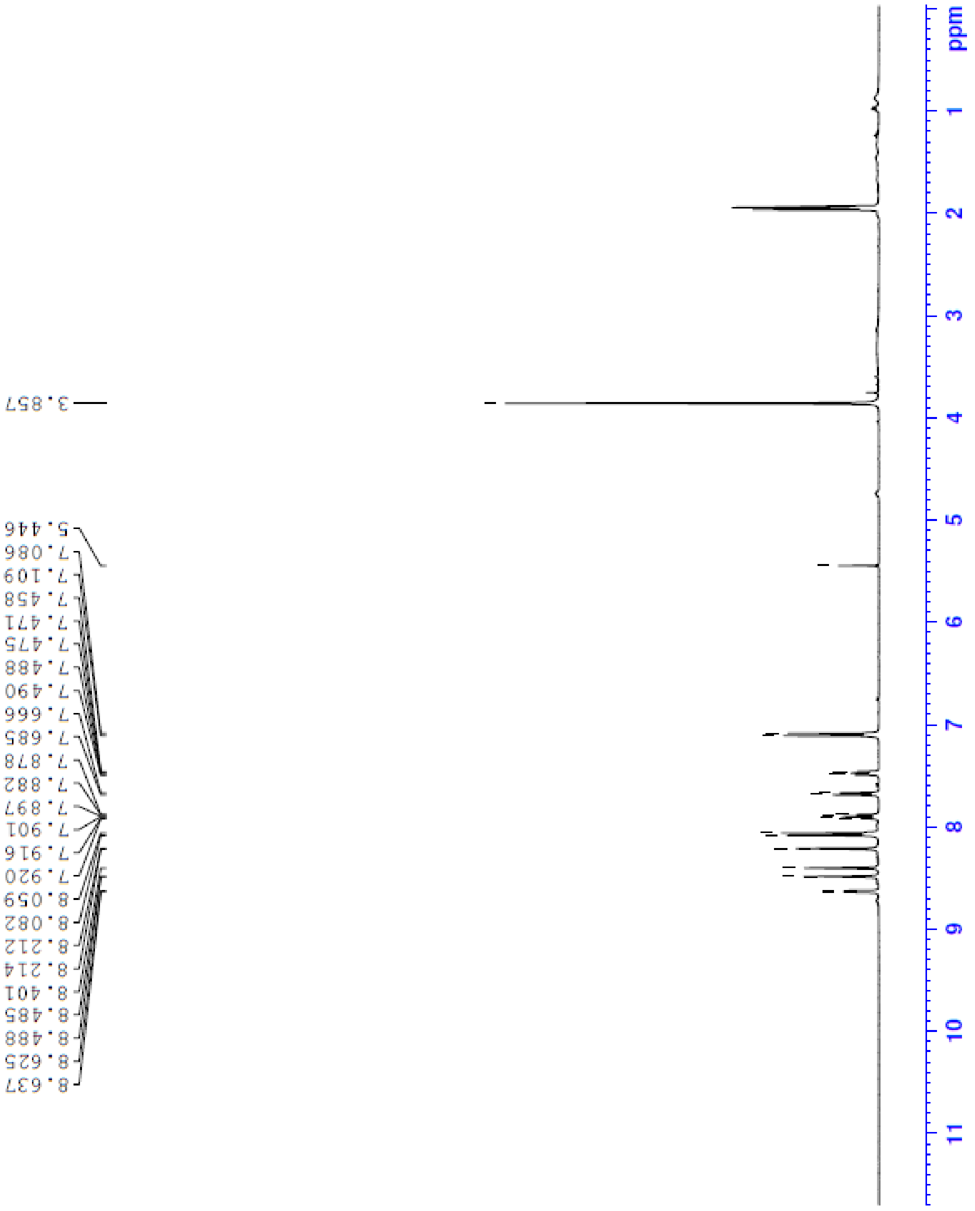
3.857
5.446
7.086
7.109
7.458
7.471
7.475
7.488
7.490
7.666
7.685
7.878
7.882
7.897
7.901
7.916
7.920
8.059
8.082
8.212
8.214
8.401
8.485
8.488
8.625
8.637
ppm
1
2
3
4
5
6
7
8
9
10
11

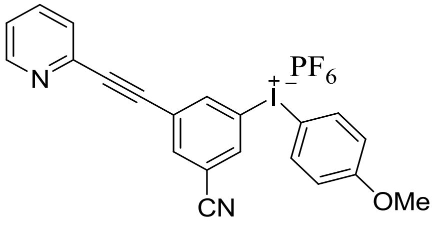
N
PF6
I
CN
OMe

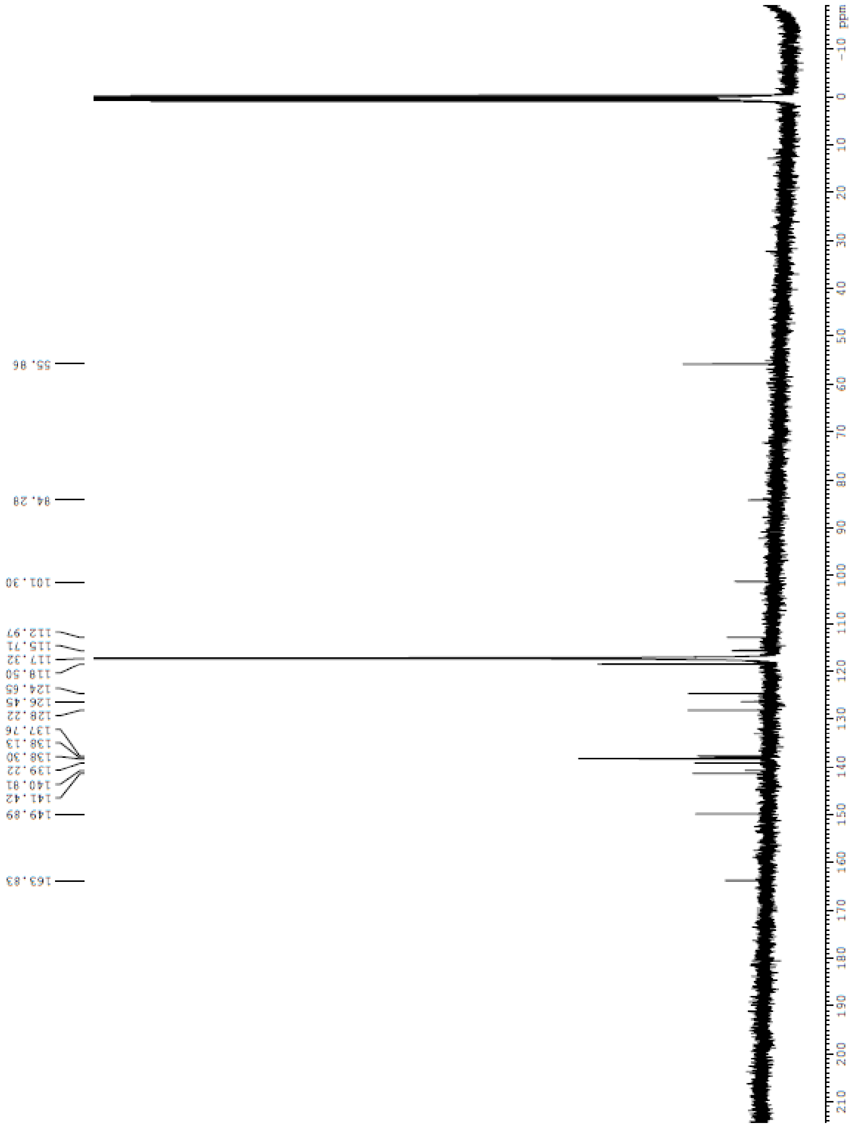
55.86
84.28
101.30
112.97
115.71
117.32
118.50
124.65
126.45
128.22
137.76
138.13
138.30
139.22
140.81
141.42
149.89
163.83
-10
0
10
20
30
40
50
60
70
80
90
100
110
120
130
140
150
160
170
180
190
200
210
ppm

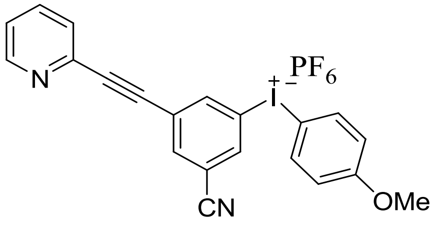
N
PF6
I
CN
OMe

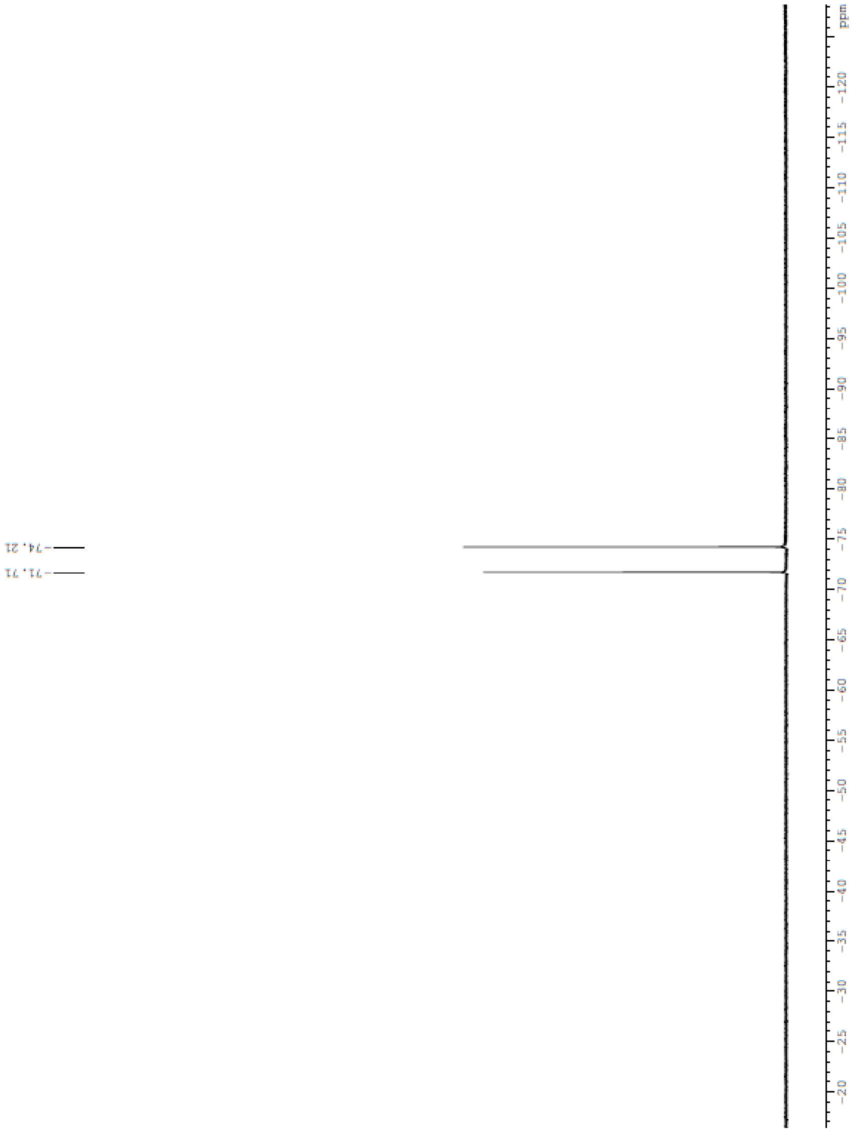
-74.21
-71.71
ppm
-120
-115
-110
-105
-100
-95
-90
-85
-80
-75
-70
-65
-60
-55
-50
-45
-40
-35
-30
-25
-20

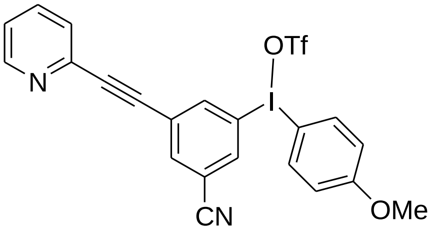
OTf
I
N
CN
OMe

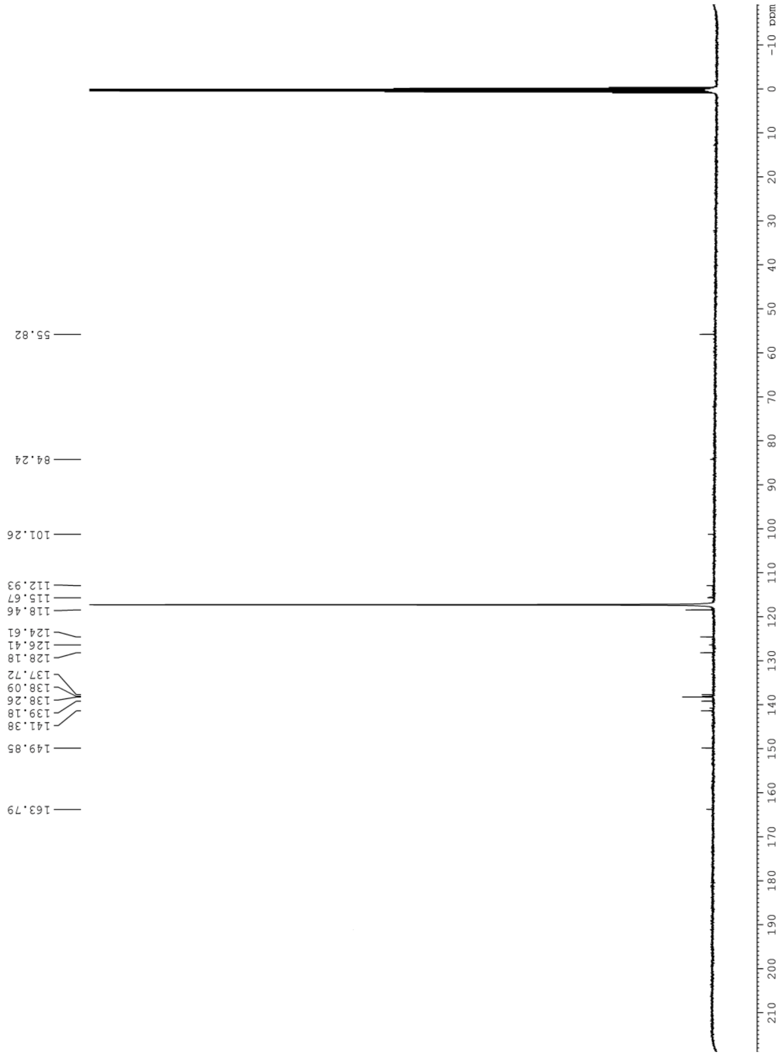
55.82
84.24
101.26
112.93
115.67
118.46
124.61
126.41
128.18
137.72
138.09
138.26
139.18
141.38
149.85
163.79
-10 ppm
0
10
20
30
40
50
60
70
80
90
100
110
120
130
140
150
160
170
180
190
200
210

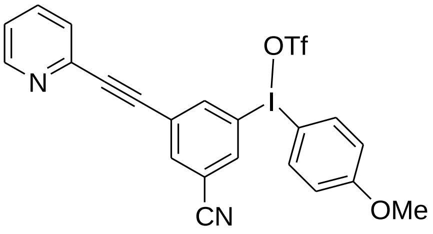
OTf
N
I
CN
OMe

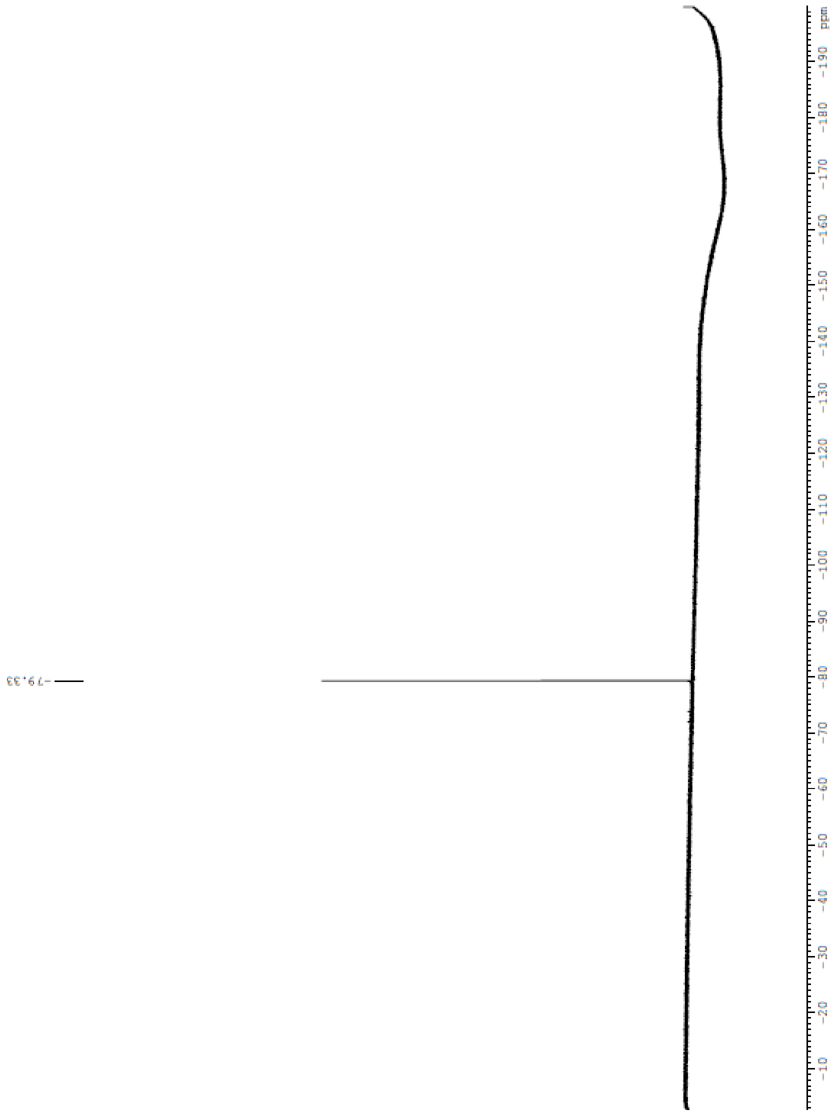
-79.33
ppm
-190
-180
-170
-160
-150
-140
-130
-120
-110
-100
-90
-80
-70
-60
-50
-40
-30
-20
-10

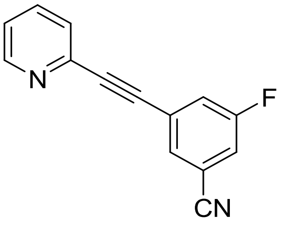
N
F
CN

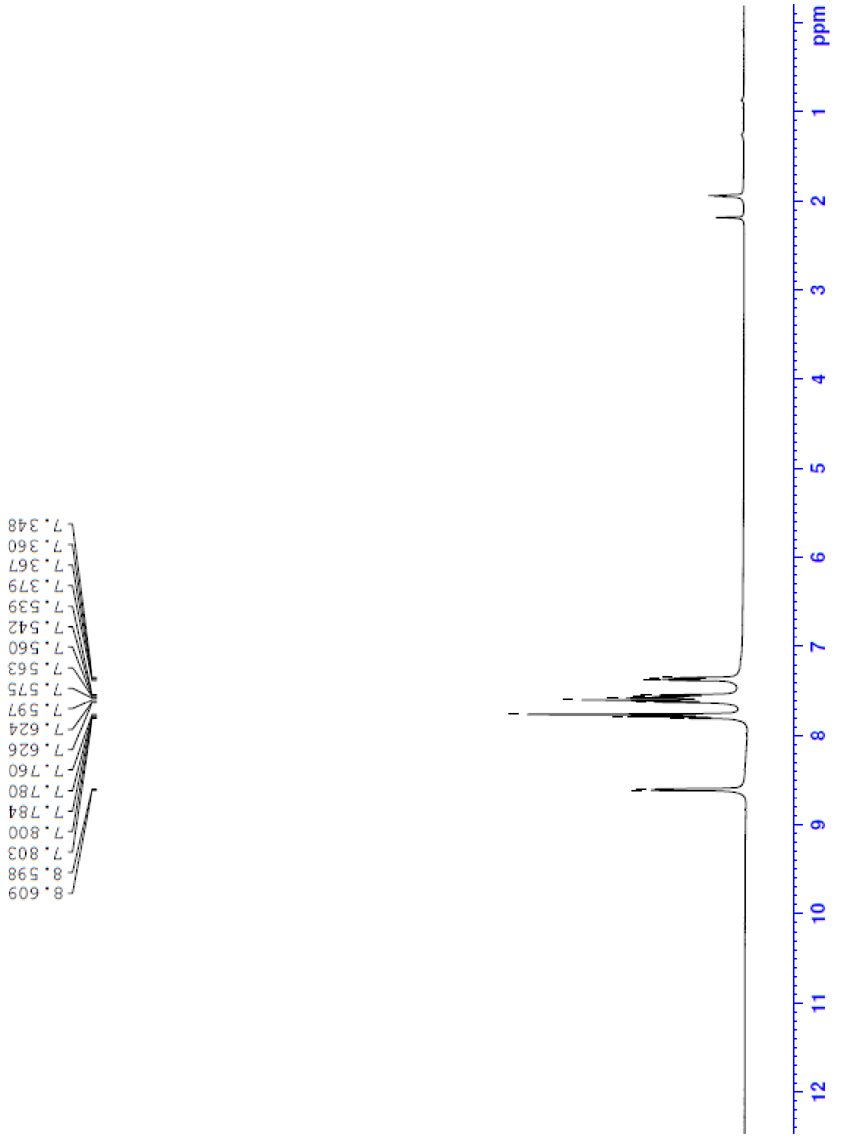
7.348
7.360
7.367
7.379
7.539
7.542
7.560
7.563
7.575
7.597
7.624
7.626
7.760
7.780
7.784
7.800
7.803
8.598
8.609
ppm
1
2
3
4
5
6
7
8
9
10
11
12

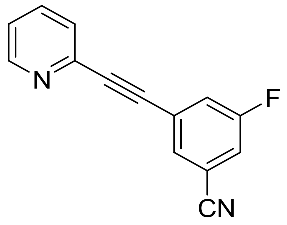
N
F
CN

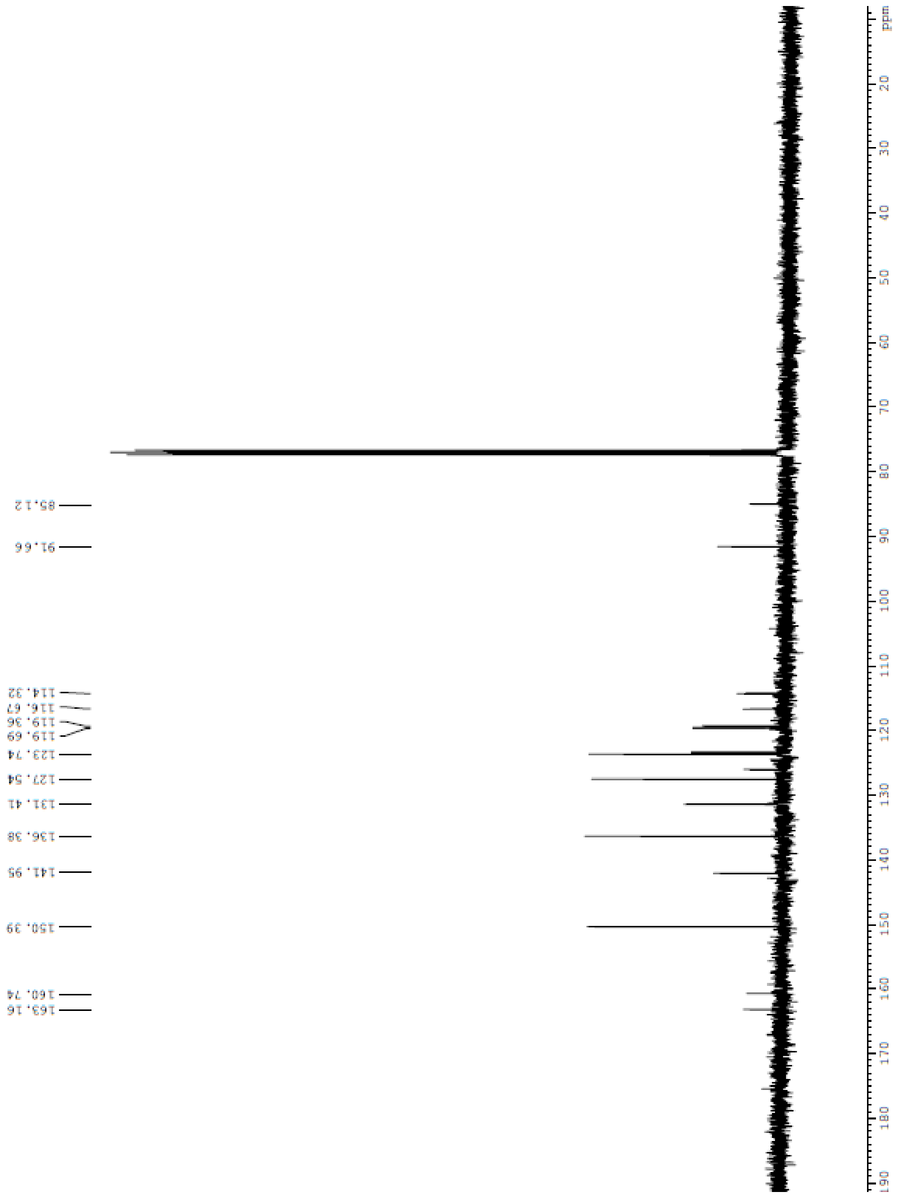
85.12
91.66
114.32
116.67
119.36
119.69
123.74
127.54
131.41
136.38
141.95
150.39
160.74
163.16
ppm
20
30
40
50
60
70
80
90
100
110
120
130
140
150
160
170
180
190

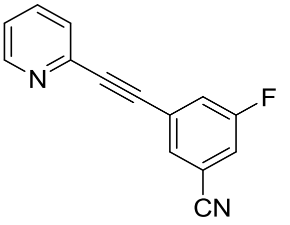
N
F
CN

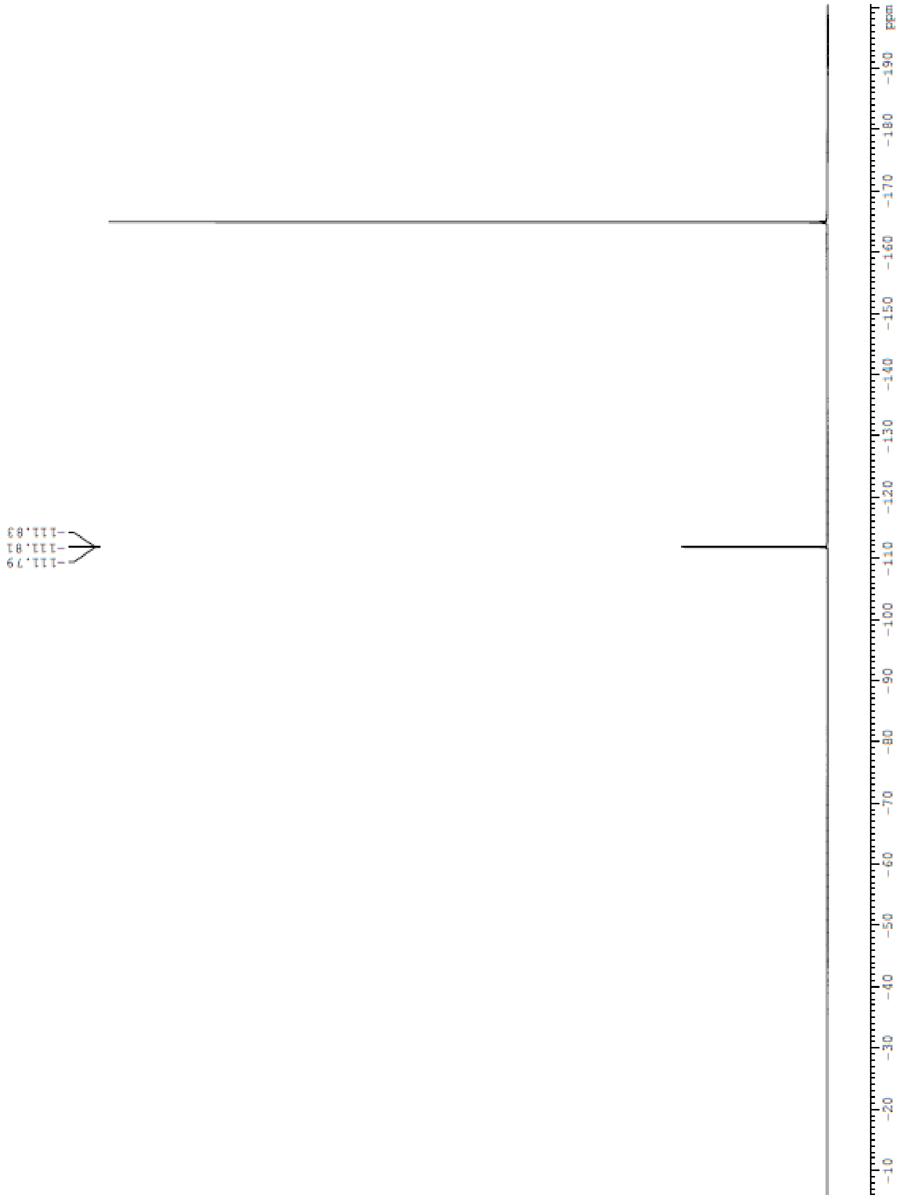
-111.83
-111.81
-111.79
ppm
-190
-180
-170
-160
-150
-140
-130
-120
-110
-100
-90
-80
-70
-60
-50
-40
-30
-20
-10

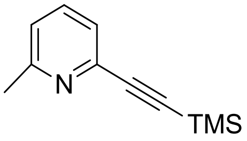
N
TMS

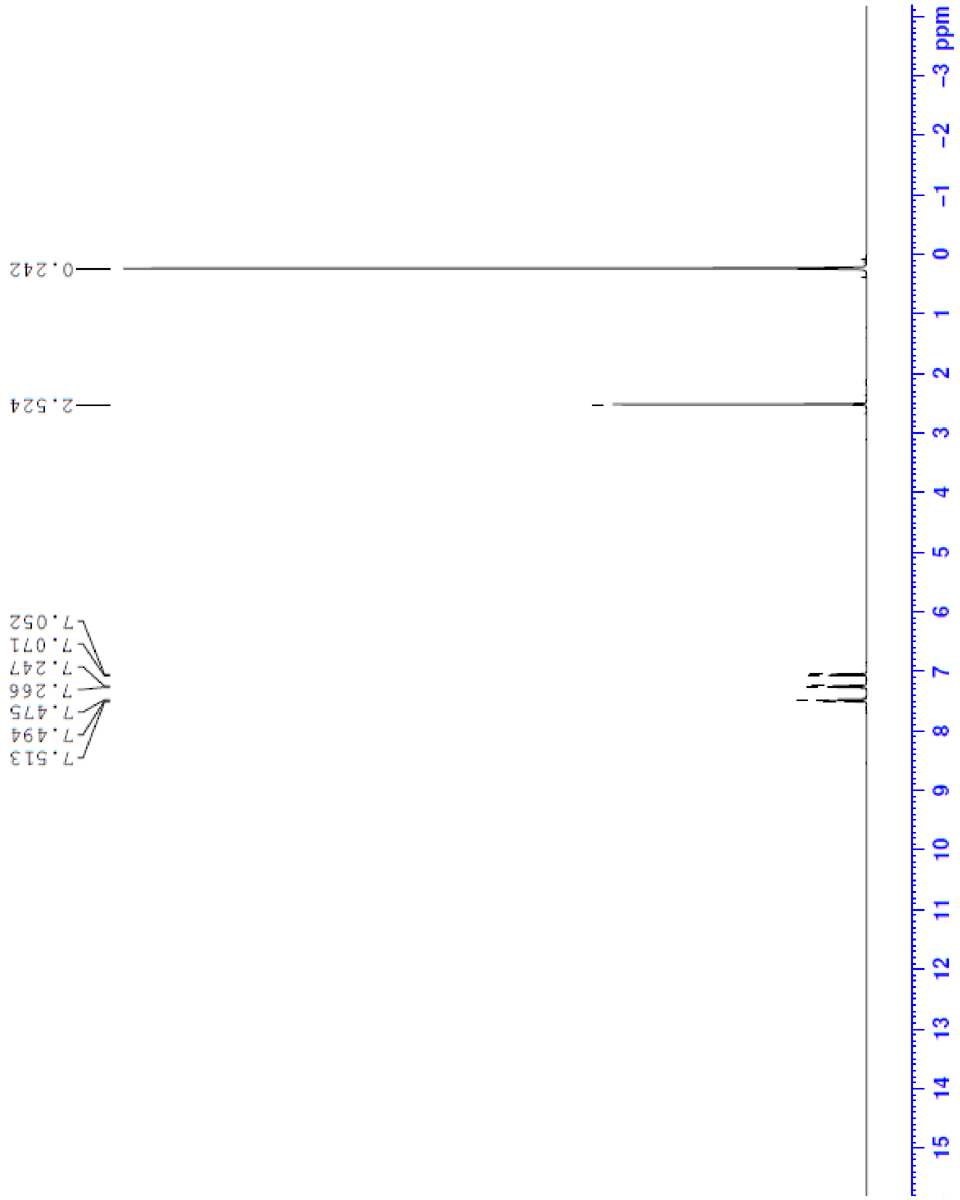
0.242
2.524
7.052
7.071
7.247
7.266
7.475
7.494
7.513
ppm
−3
−2
−1
0
1
2
3
4
5
6
7
8
9
10
11
12
13
14
15

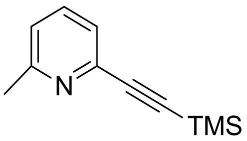
N
TMS

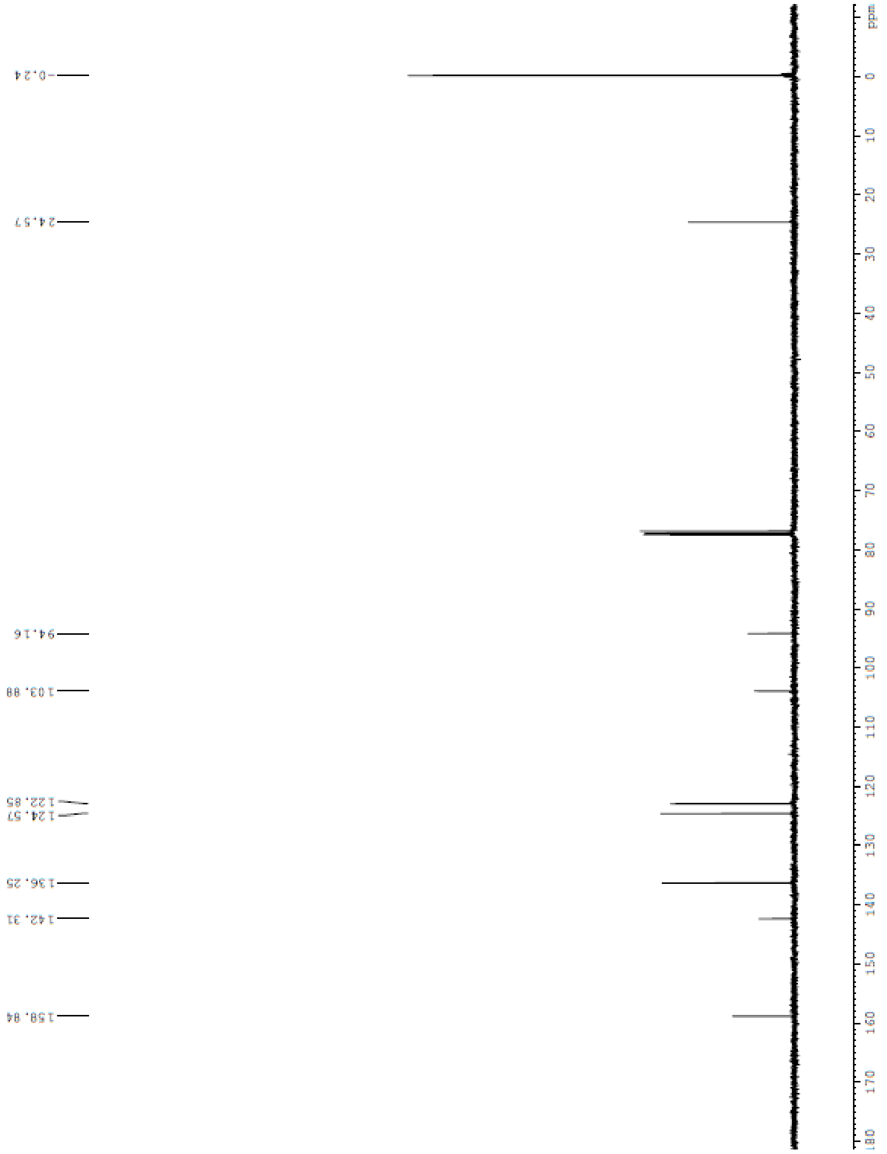
-0.24
24.57
94.16
103.88
122.85
124.57
136.25
142.31
158.84
ppm
0
10
20
30
40
50
60
70
80
90
100
110
120
130
140
150
160
170
180

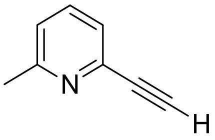
N
H

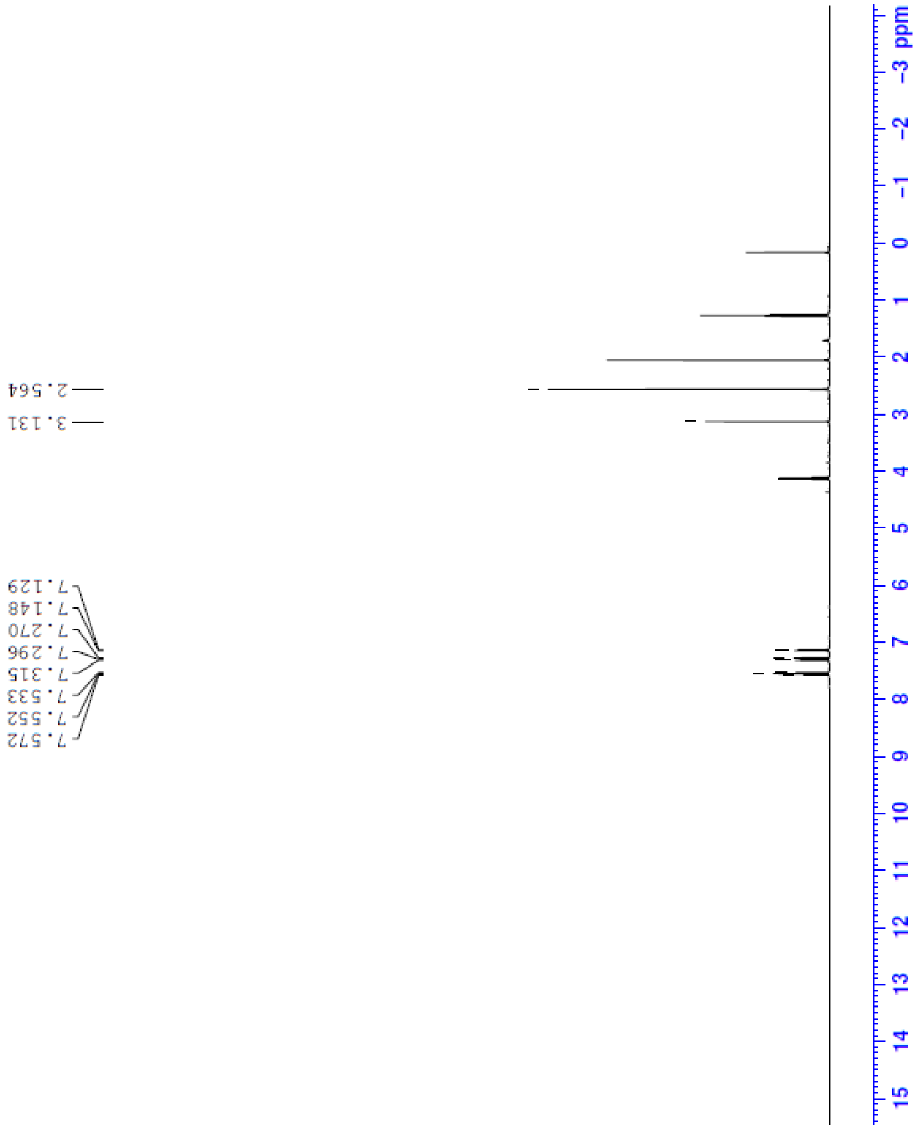
2.564
3.131
7.129
7.148
7.270
7.296
7.315
7.533
7.552
7.572
ppm
-3
-2
-1
0
1
2
3
4
5
6
7
8
9
10
11
12
13
14
15

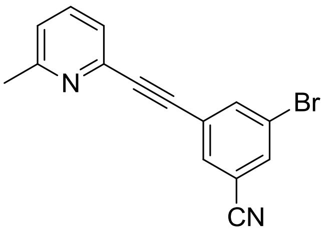
N
Br
CN

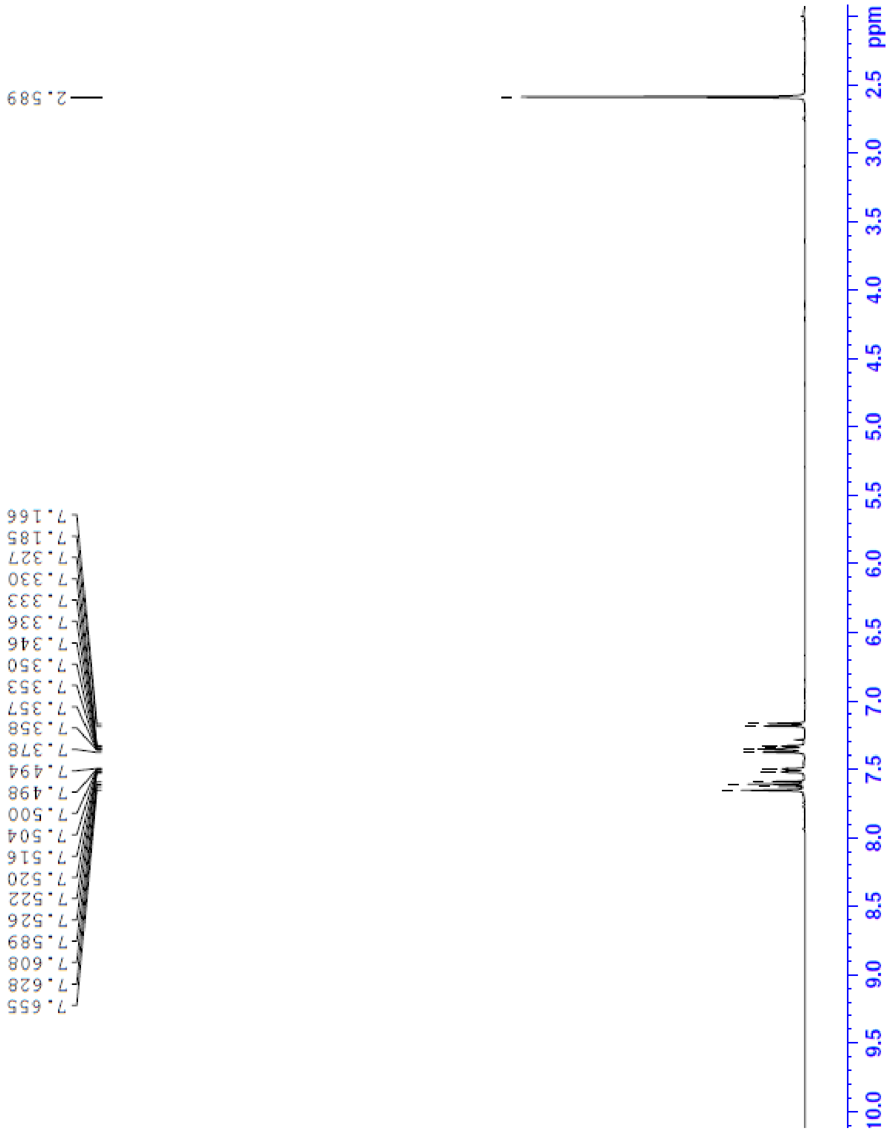
2.589
7.166
7.185
7.327
7.330
7.333
7.336
7.346
7.350
7.353
7.357
7.358
7.378
7.494
7.498
7.500
7.504
7.516
7.520
7.522
7.526
7.589
7.608
7.628
7.655
ppm
2.5
3.0
3.5
4.0
4.5
5.0
5.5
6.0
6.5
7.0
7.5
8.0
8.5
9.0
9.5
10.0

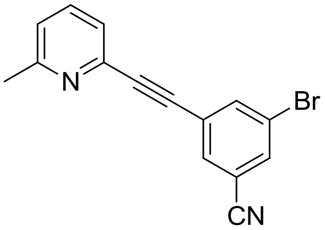
N
Br
CN

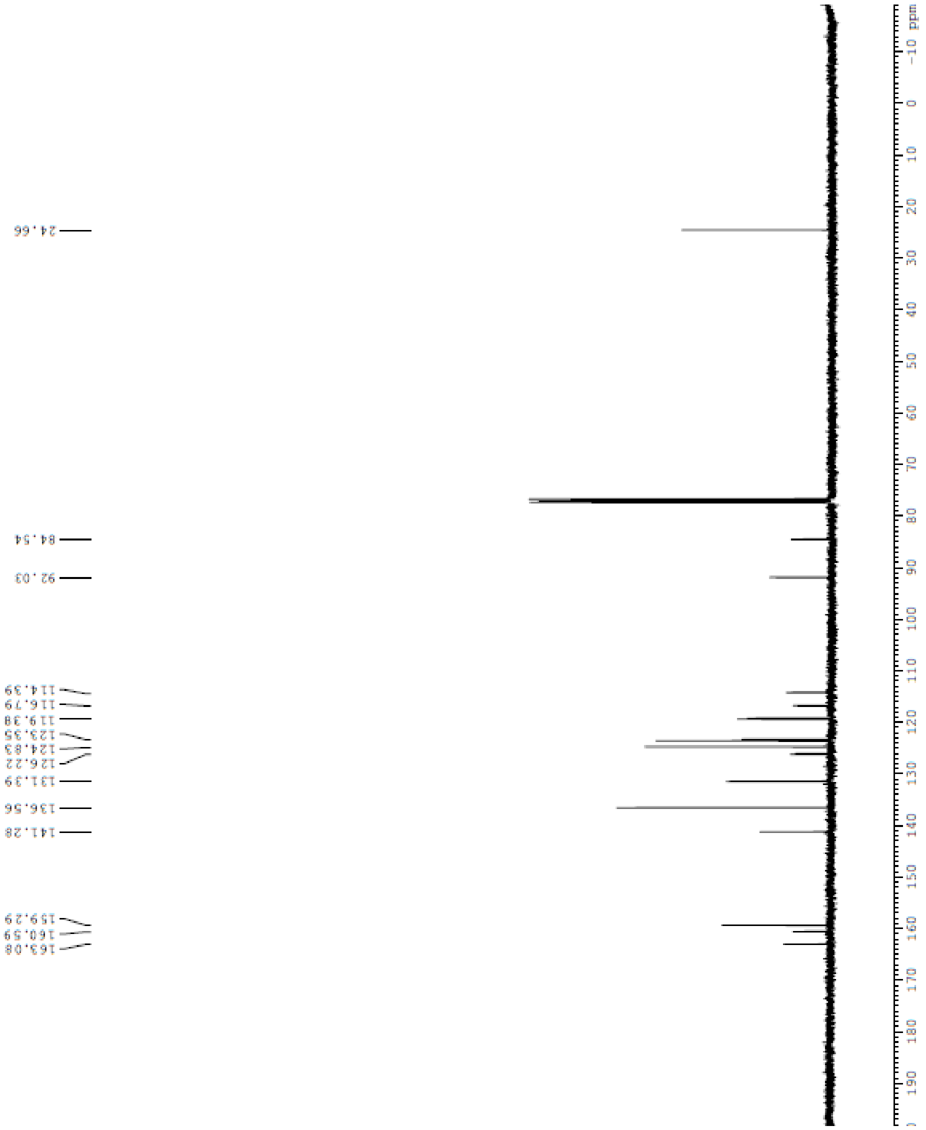
24.66
84.54
92.03
114.39
116.79
119.38
123.35
124.83
126.22
131.39
136.56
141.28
159.29
160.59
163.08
ppm
-10
0
10
20
30
40
50
60
70
80
90
100
110
120
130
140
150
160
170
180
190

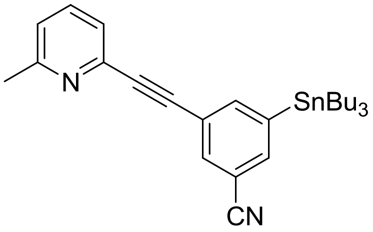
N
SnBu3
CN

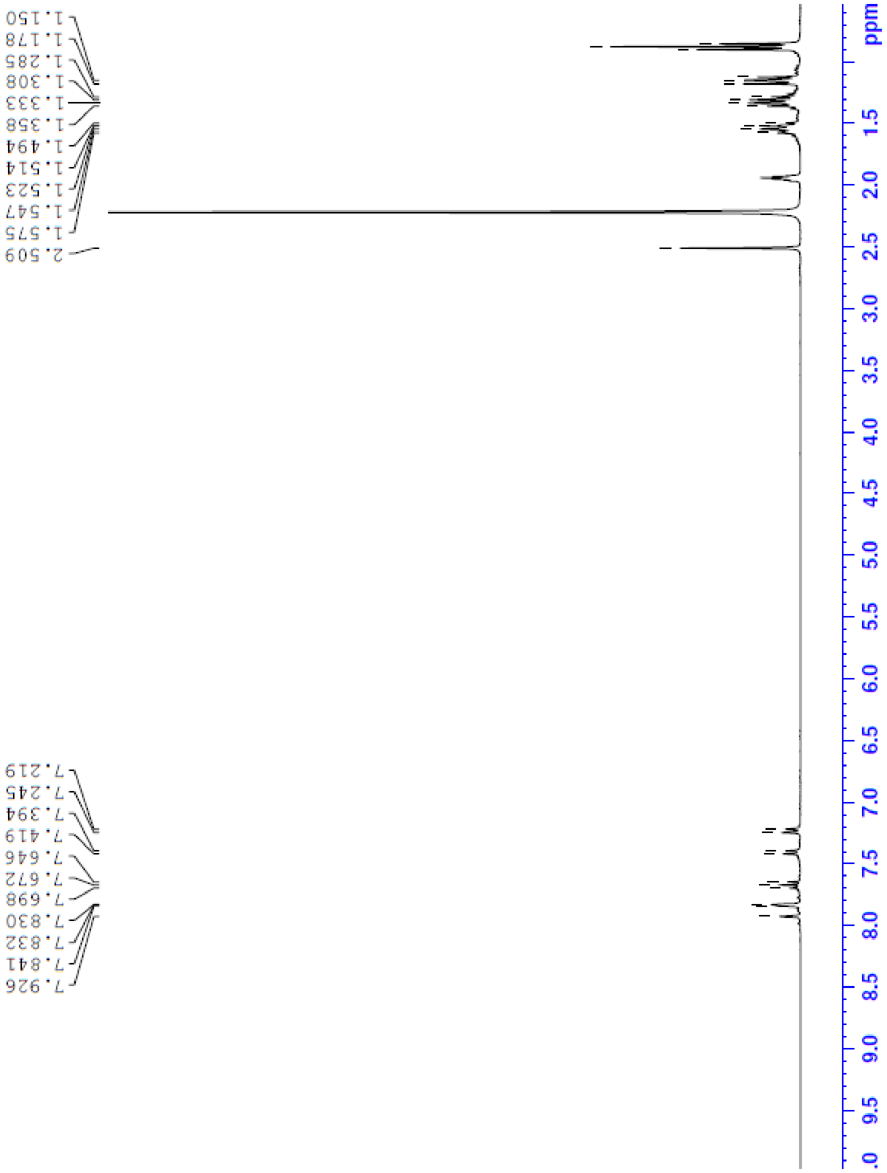
1.150
1.178
1.285
1.308
1.333
1.358
1.494
1.514
1.523
1.547
1.575
2.509
7.219
7.245
7.394
7.419
7.646
7.672
7.698
7.830
7.832
7.841
7.926
ppm
1.5
2.0
2.5
3.0
3.5
4.0
4.5
5.0
5.5
6.0
6.5
7.0
7.5
8.0
8.5
9.0
9.5
.0

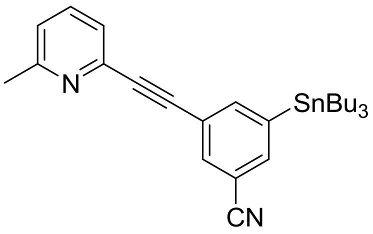
N
SnBu$_3$
CN

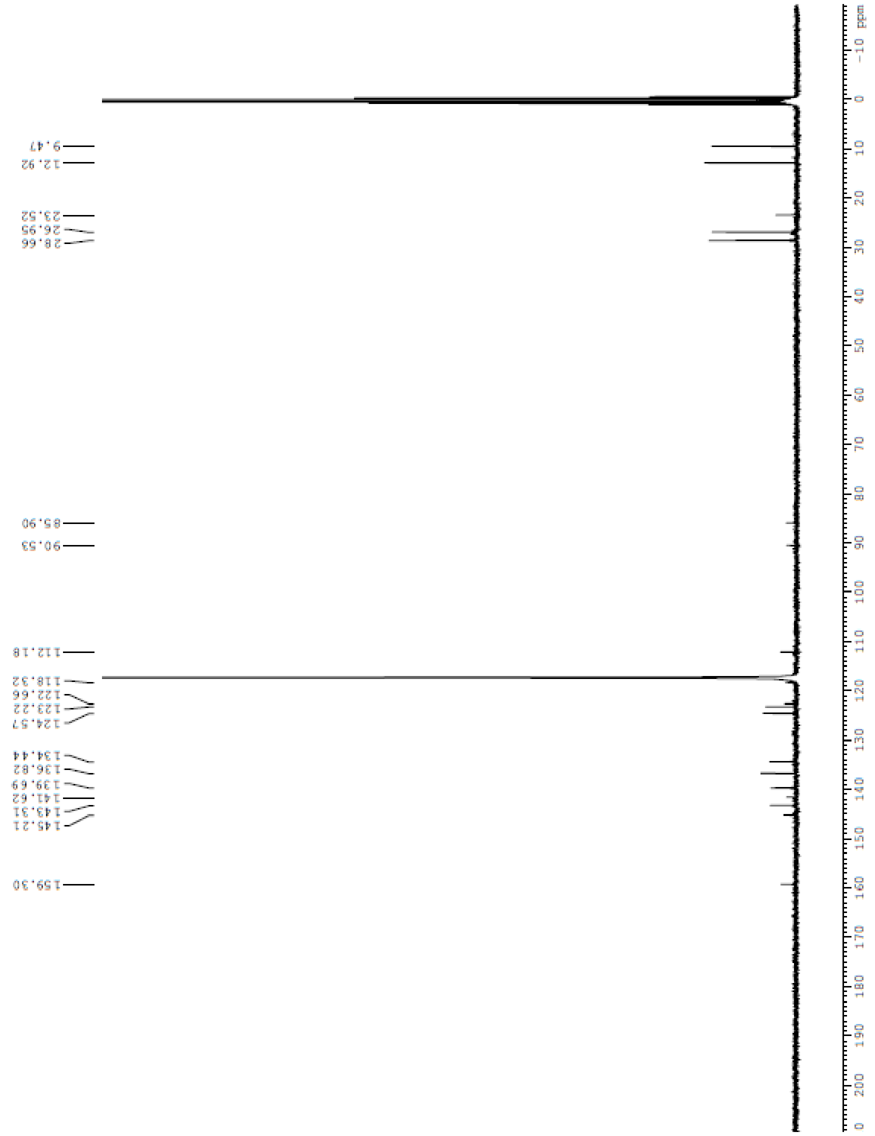
9.47
12.92
23.52
26.95
28.66
85.90
90.53
112.18
118.32
122.66
123.22
124.57
134.44
136.82
139.69
141.62
143.31
145.21
159.30
ppm
-10
0
10
20
30
40
50
60
70
80
90
100
110
120
130
140
150
160
170
180
190
200

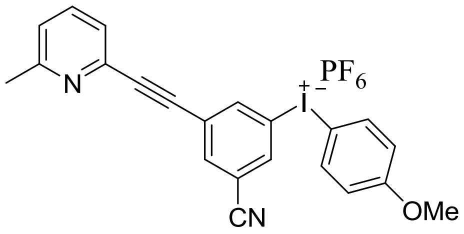
N
I
PF6
CN
OMe

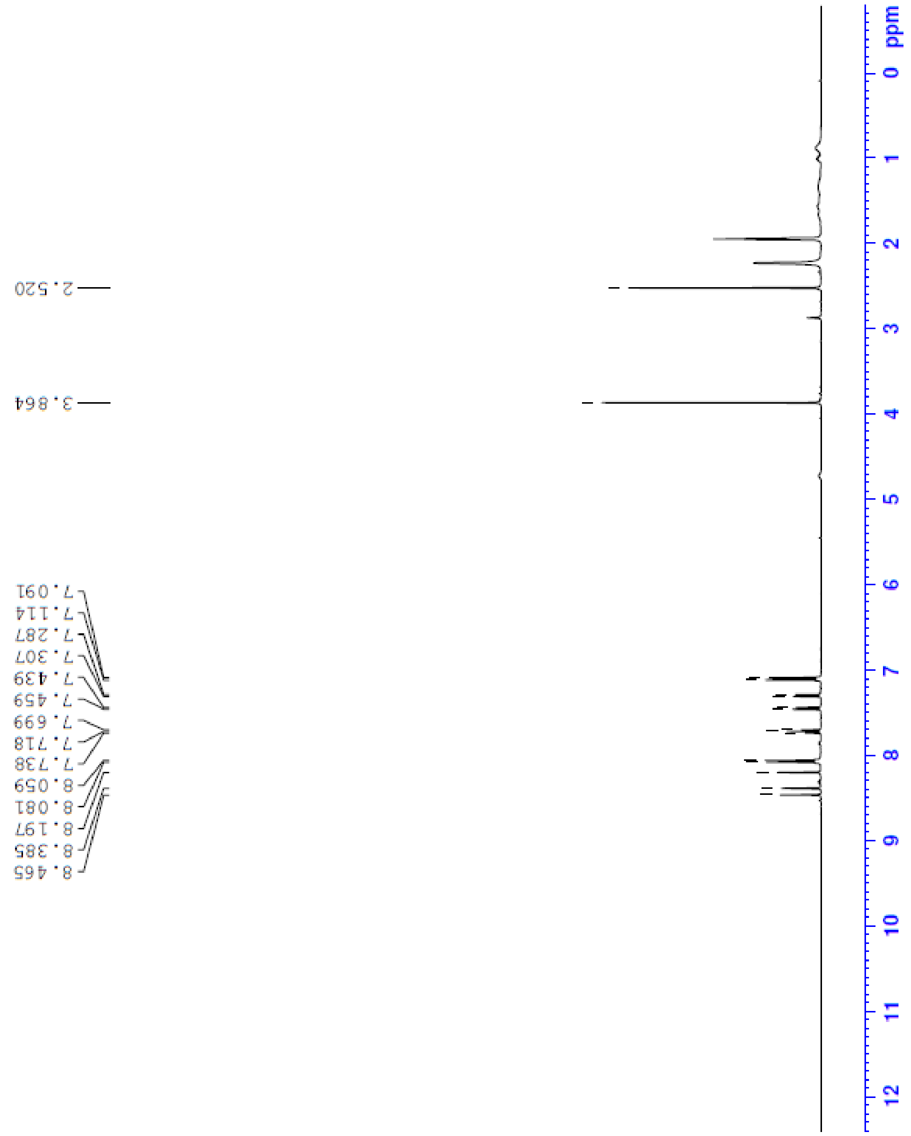
2.520
3.864
7.091
7.114
7.287
7.307
7.439
7.459
7.699
7.718
7.738
8.059
8.081
8.197
8.385
8.465
ppm
0
1
2
3
4
5
6
7
8
9
10
11
12

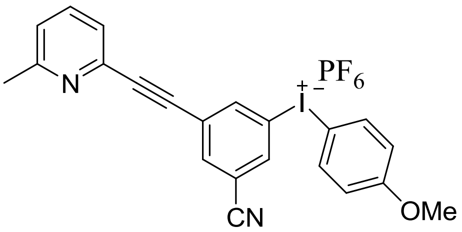
PF6
N
CN
OMe

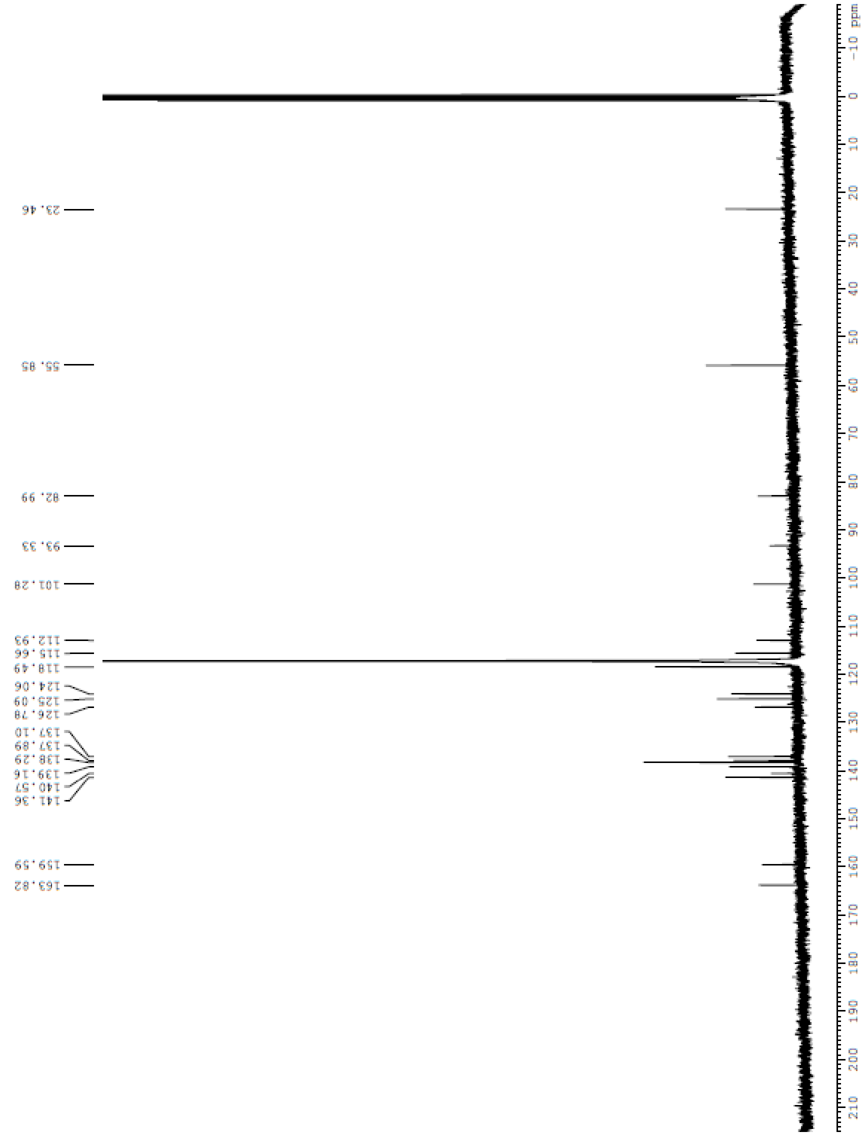
23.46
55.85
82.99
93.33
101.28
112.93
115.66
118.49
124.06
125.09
126.78
137.10
137.89
138.29
139.16
140.57
141.36
159.59
163.82
-10 ppm
0
10
20
30
40
50
60
70
80
90
100
110
120
130
140
150
160
170
180
190
200
210

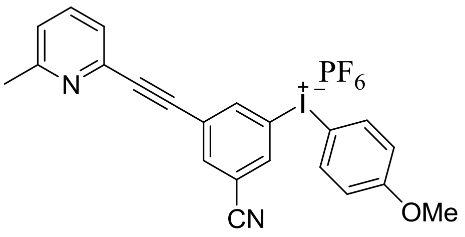
N
PF6
I
CN
OMe

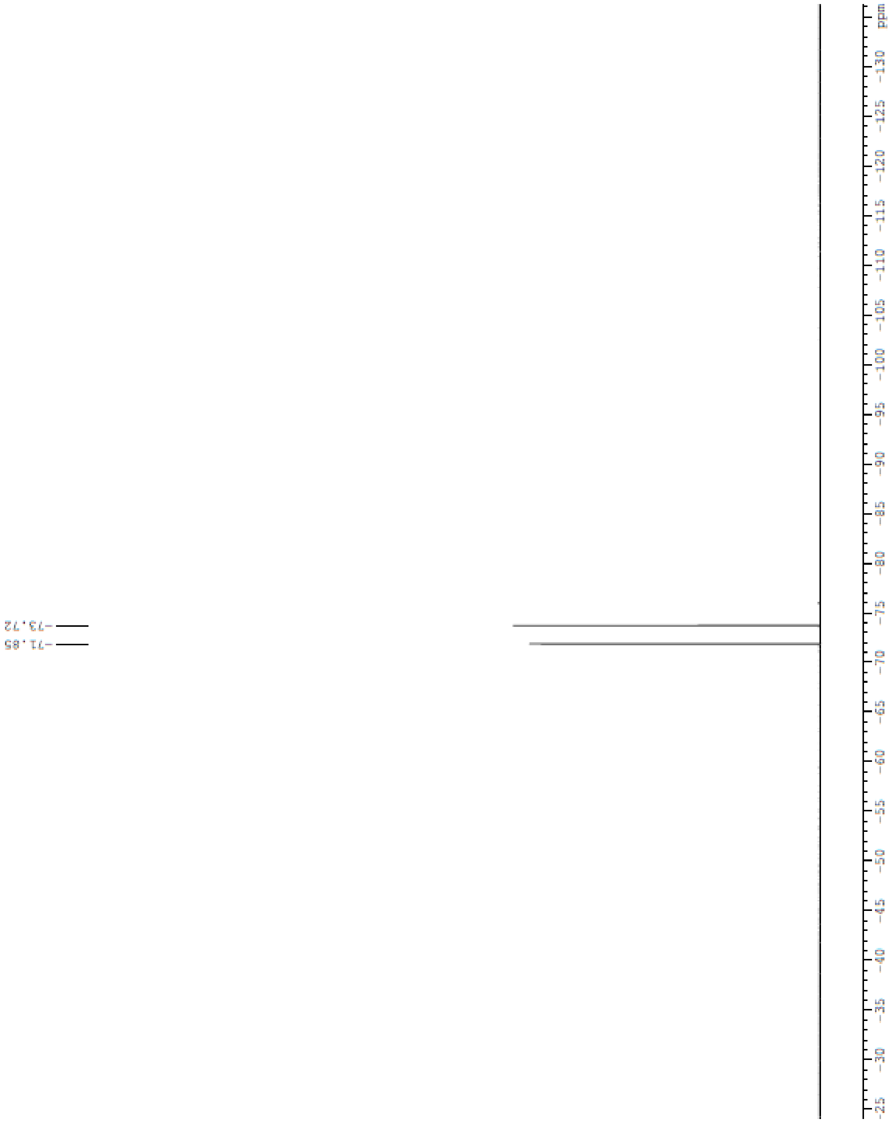
-73.72
-71.85
ppm
-130
-125
-120
-115
-110
-105
-100
-95
-90
-85
-80
-75
-70
-65
-60
-55
-50
-45
-40
-35
-30
-25

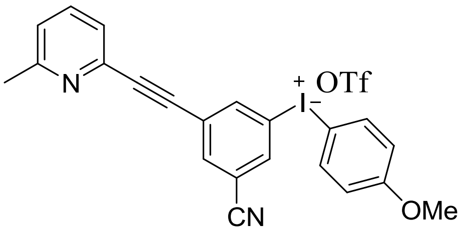
N
OTf
I
CN
OMe

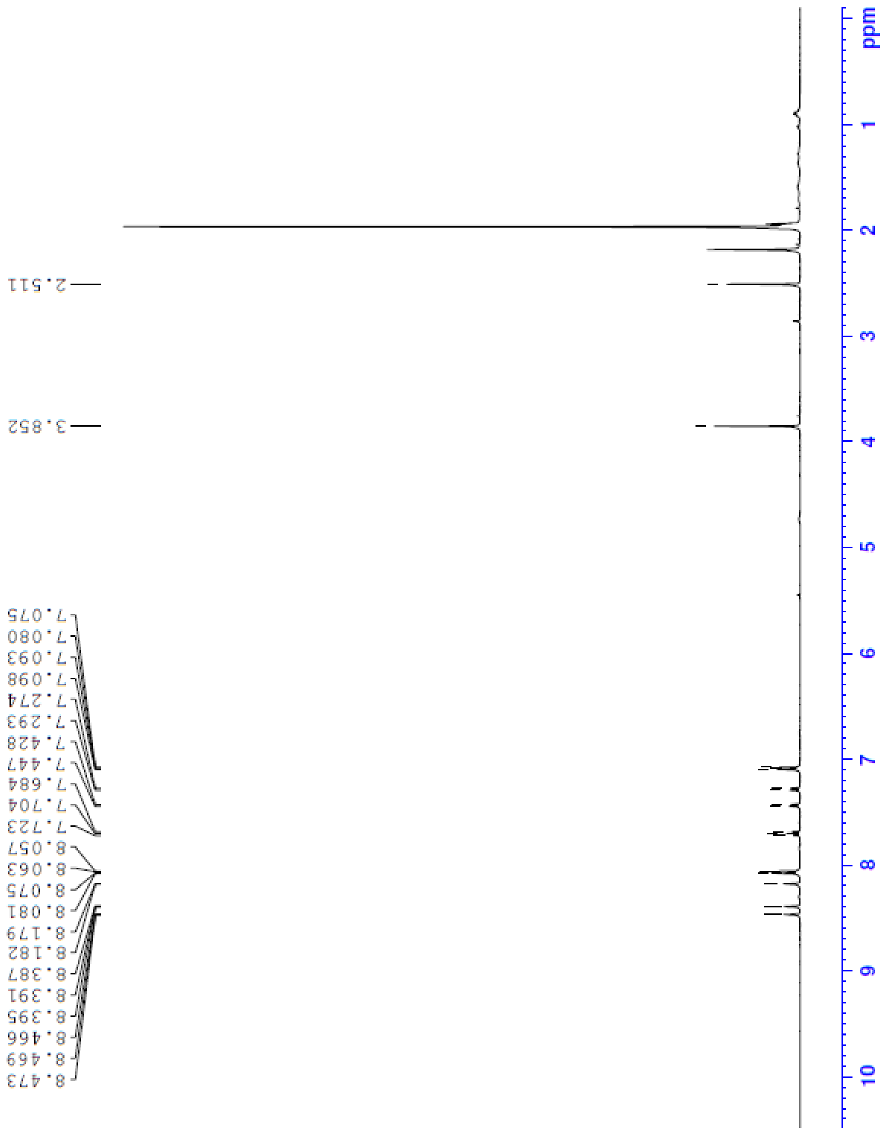
2.511
3.852
7.075
7.080
7.093
7.098
7.274
7.293
7.428
7.447
7.684
7.704
7.723
8.057
8.063
8.075
8.081
8.179
8.182
8.387
8.391
8.395
8.466
8.469
8.473
ppm
1
2
3
4
5
6
7
8
9
10

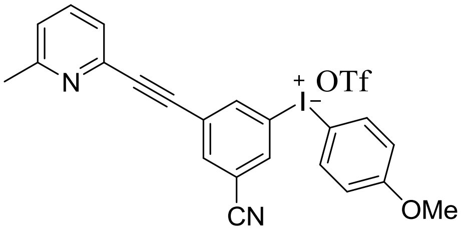
N
OTf
I
CN
OMe

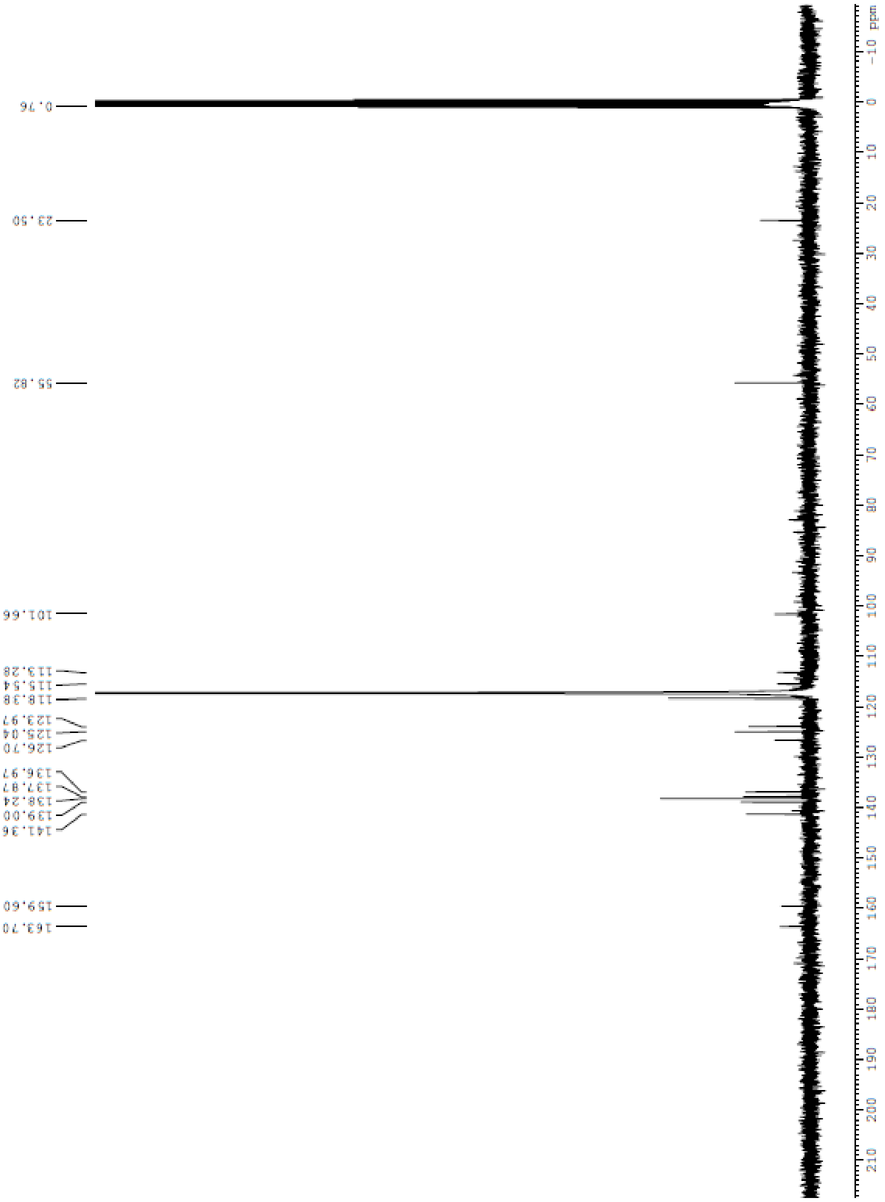
0.76
23.50
55.82
101.66
113.28
115.54
118.38
123.97
125.04
126.70
136.97
137.87
138.24
139.00
141.36
159.60
163.70
ppm
-10
0
10
20
30
40
50
60
70
80
90
100
110
120
130
140
150
160
170
180
190
200
210

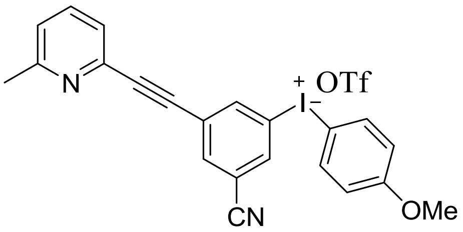
N
OTf
I
CN
OMe

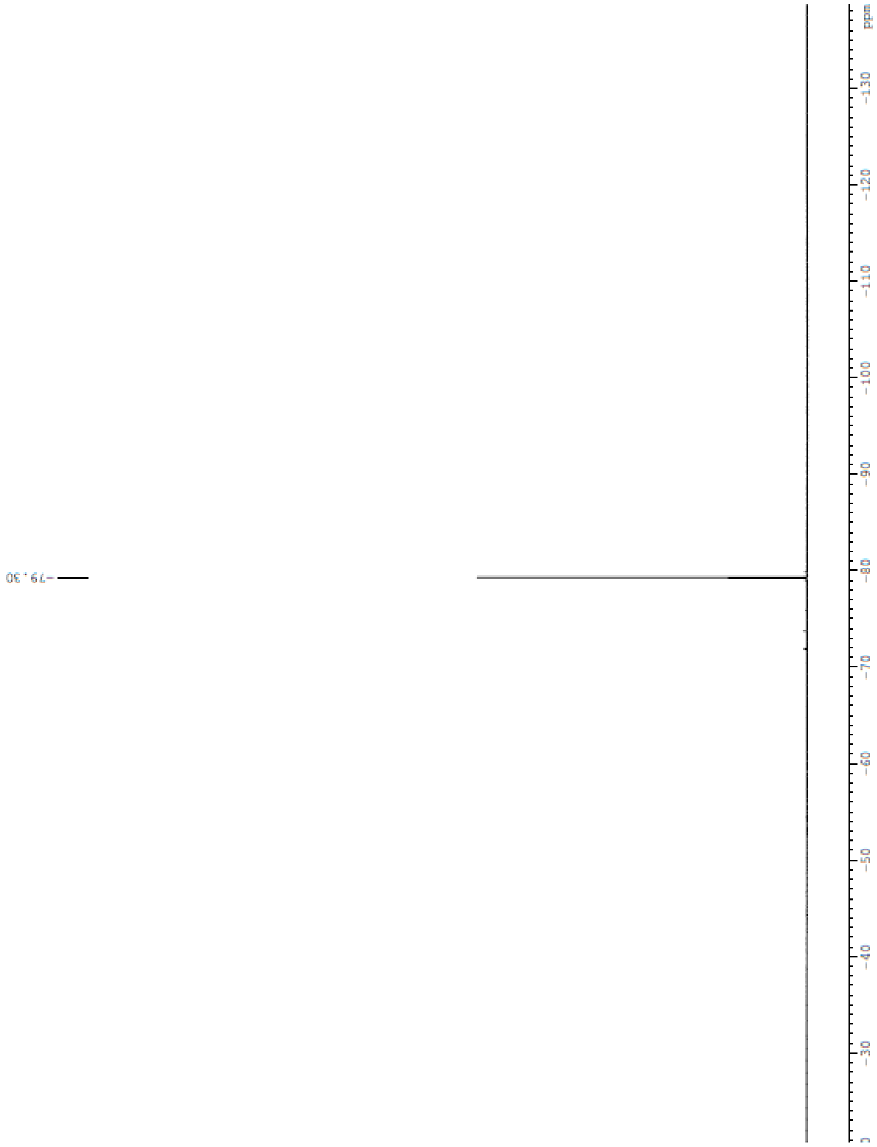
-79.30
ppm
-130
-120
-110
-100
-90
-80
-70
-60
-50
-40
-30

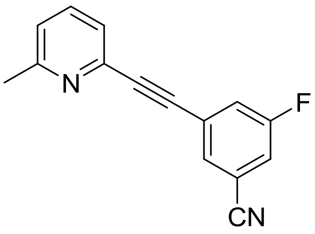
N
F
CN

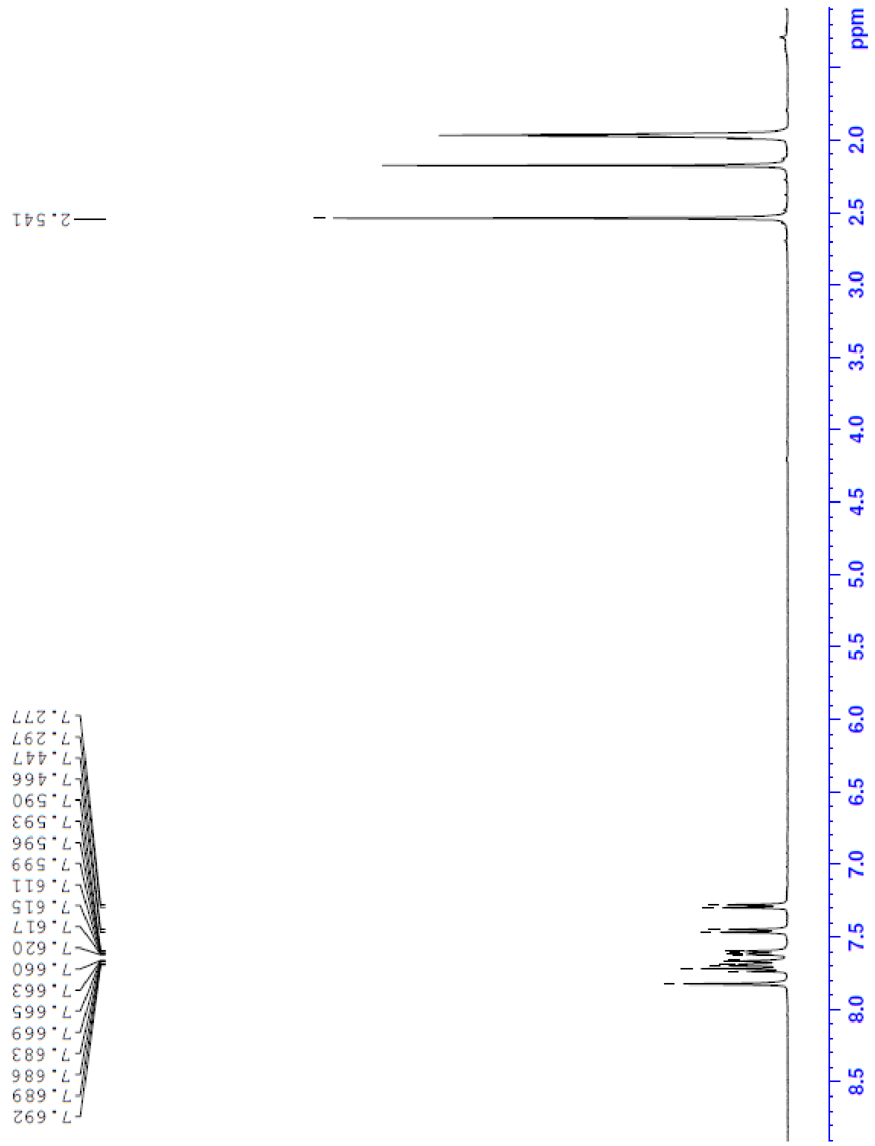
2.541
7.277
7.297
7.447
7.466
7.590
7.593
7.596
7.599
7.611
7.615
7.617
7.620
7.660
7.663
7.665
7.669
7.683
7.686
7.689
7.692
ppm
2.0
2.5
3.0
3.5
4.0
4.5
5.0
5.5
6.0
6.5
7.0
7.5
8.0
8.5

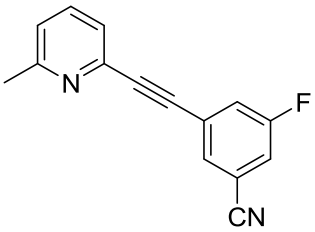
N
F
CN

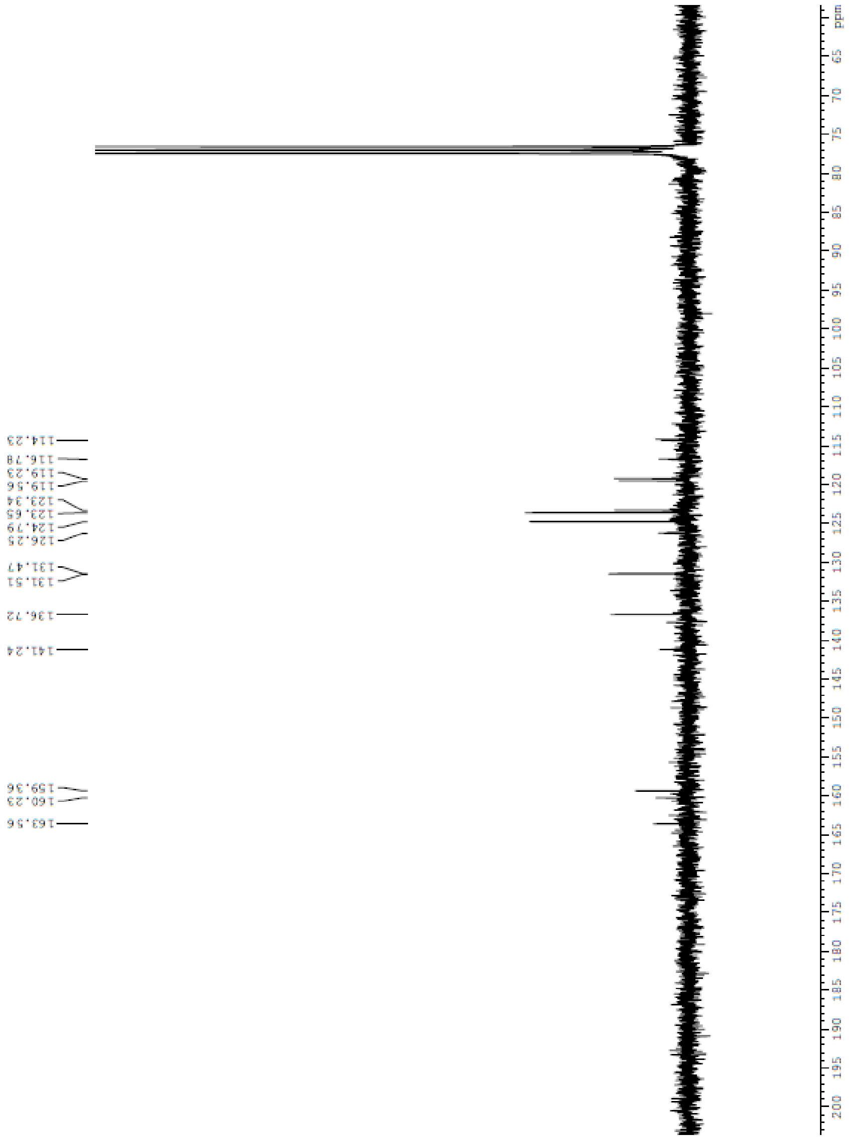
114.23
116.78
119.23
119.56
123.34
123.65
124.79
126.25
131.47
131.51
136.72
141.24
159.36
160.23
163.56
ppm
65
70
75
80
85
90
95
100
105
110
115
120
125
130
135
140
145
150
155
160
165
170
175
180
185
190
195
200

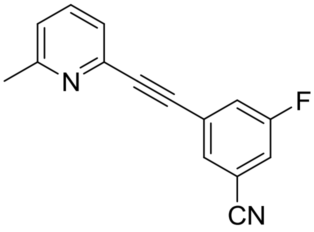
N
F
CN

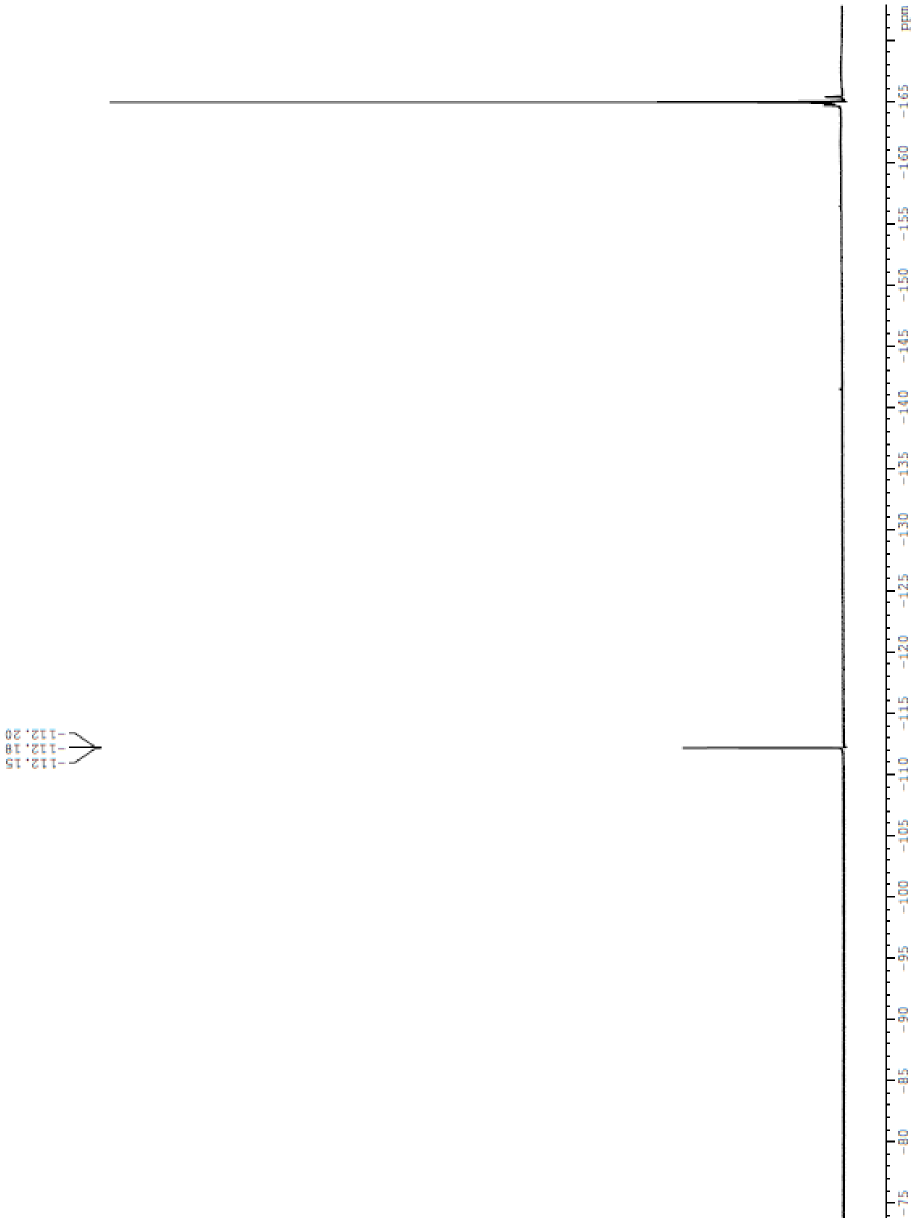
-112.20
-112.18
-112.15
ppm
-165
-160
-155
-150
-145
-140
-135
-130
-125
-120
-115
-110
-105
-100
-95
-90
-85
-80
-75